

CONFIDENTIAL

COPY NO.
RM No. E8L20

NACA RM No. E8L20



~~SECRET~~
Copy 2

RESEARCH MEMORANDUM

ALTITUDE-WIND-TUNNEL INVESTIGATION OF VARIOUS
CAN-TYPE BURNERS IN BUMBLEBEE 18-INCH RAM JET

By D. T. Dupree, T. J. Nussdorfer, and W. H. Sterbentz

Lewis Flight Propulsion Laboratory
Cleveland, Ohio

CLASSIFICATION CANCELLED

and Unavailable

Authority *NACA Res. 68* Date *5/14/56*

RN 101

By *mda 6/1/56* See

CLASSIFIED DOCUMENT

This document contains classified information affecting the National Defense of the United States within the meaning of the Espionage Act, USC 5024 and 5043. Its transmission or the revelation of its contents in any manner to an unauthorized person is prohibited by law. Information so classified may be imparted only to persons in the military and naval services of the United States, appropriate civilian officers and employees of the Federal Government who have a legitimate interest therein, and to United States citizens of known loyalty and discretion who of necessity must be informed thereof.

NATIONAL ADVISORY COMMITTEE FOR AERONAUTICS

WASHINGTON

March 16, 1949

CONFIDENTIAL



NATIONAL ADVISORY COMMITTEE FOR AERONAUTICS

RESEARCH MEMORANDUM

ALTITUDE-WIND-TUNNEL INVESTIGATION

OF VARIOUS CAN-TYPE BURNERS IN

BUMBLEBEE 18-INCH RAM JET

By D. T. Dupree, T. J. Nussdorfer
and W. H. Sterbentz

SUMMARY

An investigation on various can-type burners in a Bumblebee 18-inch ram jet under controlled conditions of pressure altitude and ram pressure ratio was conducted in the NACA Lewis altitude wind tunnel with kerosene as fuel.

The performance of the following can-type burner configurations was better than that of the other burner configurations investigated: (1) a flame holder having a two-pitch alignment of perforations, 0.07-inch-wide cooling slots, and an arrangement of fuel nozzles located within an annulus having a mean radius of 7.24 inches; and (2) a flame holder having a zero-pitch alignment of perforations, 0.16-inch-wide cooling slots, and an annulus of fuel nozzles having a mean radius of 6.69 inches.

The maximum net-thrust coefficient and minimum specific fuel consumption were obtained with the ram-jet configuration that consisted of the burner just described having a flame holder with a two-pitch alignment of perforations and a combustion-chamber outlet restricted by a $14\frac{3}{4}$ -inch-diameter orifice plate. At a ram pressure ratio equivalent to a free-stream Mach number of 1.44 and a pressure altitude of 30,000 feet, the net-thrust coefficient was 0.66 and the reduced specific fuel consumption was 3.0 pounds of fuel per hour per pound of net thrust.

INTRODUCTION

As a result of the satisfactory performance characteristics obtained from ma-level studies of a can-type flame holder in a

~~CONFIDENTIAL~~

Bumblebee 18-inch ram jet (reference 1), experiments were conducted at the NACA Lewis laboratory on **various configurations** of this **flame holder** with different fuel-injection patterns. These experiments were conducted as part of an investigation to **determine** the performance characteristics of the **Bumblebee 18-inch ram jet** primarily at **simulated conditions** of high altitudes and **ram pressure ratios** equivalent to supersonic flight **Mach numbers** (references 2 to 4). The **performance** of one combination of can-type **flame holder** and fuel-injection pattern with two fuels, kerosene and a mixture of **75-percent kerosene and 25-percent** propylene oxide, at a pressure altitude of **approximately 30,000 feet** and at **ram pressure ratios** equivalent to supersonic **flight Mach numbers** is **shown in reference 4**.

The **performance** of various can-type burners **using kerosene** (AN-F-321 fuel as influenced by changes in **flame-holder** design, fuel-injection pattern, and **combustion-chamber-outlet** area is reported herein. Also included **are** the effects of **some** of these **changes** on **such engine-performance parameters** as net-thrust coefficient and **specific fuel consumption**. The range of **simulated flight conditions investigated** generally included pressure altitudes **from 10,000 to 30,000 feet** at **ram pressure ratios** equivalent to flight **Mach numbers from 0.6 to 1.4**.

APPARATUS AND PROCEDURE

Ram jet and burners. - The **ram jet investigated** (fig. 1) is essentially the **same** as the **unit** described in **references 2 to 4**. The ram jet consists of **an annular subsonic diffuser, an 18-inch-diameter water-cooled combustion chamber, and a burner** consisting of a fuel distributor **and a flame holder**.

The installation of the fuel distributor and the can-type **flame holder** is **shown** in figure 2. The **flame holder** consists of a skirt resembling the **frustrum of a perforated segmented cone and a fuel-fed pilot forming** the vertex of the cone. Performance effects of modifications in both the skirt of the **flame holder** and the pilot were studied. Modifications to the **flame-holder skirt concerned** the size and the **alignment** of the perforations and the width of the **annular slots located under the bands** connecting the segments of the skirt. The three **modified skirts, which have zero-pitch alignment of perforations with open areas of 110, 130, and 135 percent, are shown in figures 3(a), 3(b), and 3(c), respectively.** (The pitch **alignment of the perforations is defined as the number of rows of perforations that spiral around the skirt as counted along**

1074

the intersection of an axial plane on the surface of the skirt. The percentage of open area of the skirt is defined as the ratio of the area of the perforations and slots to the cross-sectional area of the combustion chamber.) For the 110- and 130-percent open-area skirts, the width of the annular slots was 0.07 inch (figs. 3(a) and 3(b)); the difference in open area was accounted for by the change in the sizes of the perforations. For the 130- and 135-percent open-area skirts, the same size perforations were used, but an increased annular slot width of 0.16 inch was employed for the 135-percent open-area skirt (fig. 3(c)). The wide-slot skirt (135-percent open area) was shorter than the other skirts by the length of one segment ($3\frac{1}{2}$ in.). The effect of a spiral alignment of perforations around the skirt was obtained by using the skirt shown in figure 3(b), which has 130-percent open area, but is assembled with a two-pitch alignment of perforations (fig. 3(d)).

Approximately 1 percent of the total fuel flow was injected in the pilot burner of the flame holder from a commercial spray nozzle. This fuel was mixed with air that was admitted to the pilot through perforations in the pilot dome. Changing the size of the perforations and the spray nozzle, employing air scoops at the perforations, and adding air ducts to the scoops leading upstream of the main fuel injectors were methods used in an attempt to improve the performance of the pilot burner. In addition to these modifications of the standard pilot burner, the vortex pilot burner described in reference 2 was investigated. Two ducts built into the diffuser center body supplied the vortex pilot burner with air. A spray nozzle rated to deliver approximately 21.5 gallons per hour at a gage pressure of 100 pounds per square inch supplied fuel. The air was discharged in a vortex motion into the pilot burner through two 45° pipe elbows downstream of the fuel nozzle.

The low-pressure fuel-distributor system, housed in the diffuser center body (figs. 1 and 4), was designed to distribute fuel evenly to 40 fuel-injection tubes for a wide range of fuel flows (reference 5). Basic fuel patterns 3P, 4, and 4A (figs. 5(a), 5(b), and 5(c), respectively) as designated by the Applied Physics Laboratory of Johns Hopkins University, made possible variations in the over-all fuel-injection pattern by selective assembly in the fuel distributor. A value representing an average radius of all the fuel tubes is called the mean fuel radius. In figure 4, a schematic diagram is shown for a typical over-all fuel-injection pattern. The fuel used was m-F-32, hereinafter designated kerosene, and was injected in an upstream direction.

Installation and procedure. - The rsm-jet installation in the altitude wind tunnel, more fully described in references 2 to 4, is shown in figure 6. During part of the investigation, the $17\frac{1}{2}$ -inch diameter of the combustion-chamber outlet was restricted by a $14\frac{3}{4}$ -inch-diameter orifice plate. A duct supplied the engine with dry air that could be throttled from sea-level pressures to the desired combustion-chamber-inlet pressure at a temperature of $140^{\circ} \pm 10^{\circ}$ F. Inserted between the air duct and the ram-jet-diffuser inlet was a sealed slip joint that allowed free movement of the model and use of the tunnel balance system to measure thrust. Inasmuch as the ram jet exhausted directly into the tunnel test section, changes in ram pressure ratio across the engine could be obtained by variation of either the engine-inlet pressure or the tunnel pressure altitude.

From total pressures, static pressures, and indicated temperatures measured with a survey rake in the air duct at the slip joint (figs. 1 and 6), air flowthrough the engine was computed. The air flow and the wall static pressures measured at the combustion-chamber inlet (station 2, fig. 1) were used to compute combustion-chamber-inlet velocities. As an alternate to the tunnel balance system, water-cooled combustion-chamber-outlet-rake data of total and static pressures were occasionally used to calculate jet thrust. From two total-pressure rakes mounted immediately upstream and downstream of the fuel-injector tubes, the radial profile of air flow in the diffuser and at the combustion-chamber inlet was determined. Fuel-flow measurements were made with a rotameter.

All computations of combustion and engine performance were made by methods outlined in references 6 and 7. Combustion efficiency and total-temperature ratio across the engine included the heat lost to the combustion-chamber cooling water. The pressure loss that would occur across a normal shock at the throat of a convergent-divergent diffuser of optimum contraction ratio was added to the measured diffuser-inlet total pressure and the sum was used as equivalent free-stream total pressure in the computation of equivalent free-stream Mach number.

Data were obtained at pressure altitudes from 10,000 to 30,000 feet over a range of combustion-chamber-inlet static pressures and operable fuel-air ratios. When possible, lean and rich fuel-air ratio blow-out points were determined.

SYMBOLS

The following symbols **are** used in this report:

A	cross-sectional area, square feet
C_F	net-thrust coefficient, $\frac{F_n}{\frac{1}{2}\rho_0 V_0^2 A_3}$
F_j	jet thrust, pounds
F_n	net thrust, pounds
f/a	fuel-air ratio
M	Mach number
P	total pressure, pounds per square foot absolute
P	static pressure, pounds per square foot absolute
q	dynamic pressure , pounds per square foot
T	total temperature , °R
V	velocity, feet per second
W_f	fuel flow , pounds per hour
Y	ratio of specific heat at constant pressure to specific heat at constant volume
δ	ratio of absolute tunnel ambient-air pressure to absolute static pressure at NACA standard atmospheric conditions at sea level, $p_0/2116$
η_b	combustion efficiency, percent
θ	ratio of absolute total temperature at diffuser inlet to absolute static temperature at NACA standard atmospheric conditions at sea level, $T_1/519$
ρ	density, slugs per cubic foot

T ratio of **absolute total temperature** at **combustion-chamber outlet** to absolute **total temperature** at diffuser inlet, T_4/T_1

Subscripts:

0 equivalent **free-stream** condition
 1 **subsonic diffuser inlet**
 2 **subsonic diffuser outlet and combustion-chamber inlet**
 3 Outlet Of **combustion chamber** Of **constant cross-sectional area (18-in. diam)**
 4 ram-jet **outlet**
 J **exhaust jet at ambient pressure** ($p_j = p_0$)

Performance parameters:

$F_j/8$ **jet thrust reduced to NACA standard atmospheric conditions at sea level, pounds**

$W_f / F_n \sqrt{\theta}$ **reduced specific fuel consumption, pound8 fuel per hour per pound net thrust**

RESULTS AND DISCUSSION

Ram-Jet Combustion Performance

Operational performance of burners. - The configurations investigated and the approximate range of **combustion-chamber-inlet variables** over which the engine **was** operated **are shown** in table I. The **investigation** began with a study of the **performance of a burner** (configuration 1, table I) employing the **flame holder** having **130-percent open area, zero-pitch alignment** of perforations, and a **cooling-slot width** of 0.07 inch. Alternately **spaced fuel patterns 4 and 3P**, with tube 5 of pattern 3P **plugged**, provided fuel distribution. This fuel-injection **arrangement** gave a mean fuel radius of **7.20 inches**. In general, **combustion** could be **characterized** as rough over **most** of a **narrow range** of operable **fuel-air ratio**8 (0.060 to 0.080). Flame blow-out occurred before choking could be obtained at the **combustion-chamber outlet**.

Improvement in the range of operation of this configuration was attempted by decreasing the flame-holder open area to 110 percent through a reduction in the size of the perforations (configuration 2, table I). This change, however, caused a decrease in the fuel-air-ratio operating range (0.068 to 0.078).

In order to determine the effect of a change in the mixing of the burned and unburned gases in the region of the flame holder, a two-pitch alinement of perforation8 in the burner used in configuration 1 was studied (configuration 3, table I). Some improvement in combustion stability and fuel-air-ratio operating range (0.041 to 0.083) over configuration 1 was obtained. Flame blow-out again occurred before the engine could be choked.

Inasmuch as the widest operable range of fuel-air ratio had been obtained with the two-pitch flame holder having 130-percent open area, the effect8 that a change in the fuel-distribution pattern would have on the performance of this flame holder were determined. Configuration 4 of table I employs this flame holder in conjunction with a fuel injector composed of alternately spaced fuel patterns 4 and 3P with no tube8 plugged and a mean fuel radius of 6.89 inches. A deterioration of combustion stability and narrowing of fuel-air-ratio operable range indicated that a larger mean fuel radius should be investigated. The operable range of fuel-air ratio8 was from 0.050 to 0.069.

When tubes 1 and 5 in pattern 3P were plugged and the mean fuel radius thereby increased to 7.24 inches, the ram jet could be choked and stable combustion over a wide range of operating condition8 was obtained. This burner performance was thoroughly investigated both with and without a $1\frac{3}{4}$ -inch-diameter orifice plate attached to the combustion-chamber outlet (configurations 5 and 6, respectively, table I) and will be subsequently discussed. Hereinafter the designation of burner configurations 5 and 6 (table I) will be the two-pitch 8standard-slotburner.

A narrower operable range of fuel-air ratio8 was obtained when the mean fuel radius was increased to 7.37 inches by replacing patterns 3P with fuel pattern 44, tube8 1 and 2 plugged, (configuration 7, table I). Flame blow-out occurred at fuel-air ratio8 leaner than about 0.075 and richer than about 0.092. The ram jet could be choked with thi8 burner configuration.

Although unsatisfactory combustion-chamber performance was obtained when fuel patterns 4 and 3P were used with the two-pitch

standard-slot flame holder (configuration 4, table I), satisfactory results were obtained when this fuel-injection pattern was employed with the flame holder having 135-percent open area, zero-pitch alignment, and 0.16-inch cooling slot. With this burner (configuration 8, table I, hereinafter called the zero-pitch wide-slot burner), the unit could be choked and would burn smoothly over a wide range of fuel-air-and ram pressure ratios.

Various changes made in the pilot burner had no discernable effect on the combustion performance of the main burner. Some changes, however, caused difficulty in igniting both pilot and main burner at high values of combustion-chamber-inlet velocity. The least ignition difficulties were experienced with a pilot burner, which had a perforated dome fitted with air scoops.

Effect of combustion-chamber-inlet conditions on operational limits. - The fuel-air-ratio operational limits of combustion as a function of combustion-chamber-inlet velocity V_2 and static pressure p_2 for the two-pitch, standard-slot burner both with and without the orifice plate attached to the combustion-chamber outlet are shown in figure 7(a) and 7(b), respectively. The orifice plate was used in order to obtain burner performance over a wide range of V_2 . Tailed data points in figure 7 represent choking at the ram-jet outlet. Solid curves are faired through data points having approximately the same values of p_2 and ram pressure ratio across the engine. Scatter in the data having constant p_2 would be expected and was observed where the ram pressure ratio across the engine was not held constant. The approximate conditions of fuel-air ratio and V_2 at which flame blow-out was observed are indicated by the dashed curves.

With the orifice plate attached to the combustion chamber (fig. 7(a)), the operable range of fuel-air ratio at a V_2 of 130 feet per second extended from a lean limit of about 0.045 to a rich limit greater than 0.12. As V_2 was increased to about 135 feet per second and p_2 was decreased to 1400 pounds per square foot absolute, the rich limit decreased sharply to 0.10. Further increases in V_2 to about 170 feet-per second caused only a very small change in the fuel-air-ratio blow-out limits. Choking at the outlet of the orifice plate prevented attainment of V_2 greater than about 185 feet per second.

The extension of this plot of operational limits as a function of V_2 is presented in figure 7(b) for the ram jet without the orifice plate. A comparison of fuel-air-ratio limits at the same V_2 reveals little change in these limits when the orifice plate was removed. As V_2 was increased from 180 to 190 feet per second, a decrease in operating range occurred at the lean limit, the fuel-air-ratio blow-out limit changing from 0.050 at 180 feet per second to 0.064 at 190 feet per second. Beyond these limits of f/a and V_2 was a region in which combustion was unpredictable, rough, and unstable. This region appeared to be limited by a curve extending from a fuel-air ratio of 0.040 at a V_2 of 185 feet per second to 0.065 at 198 feet per second. Further increases in V_2 from 190 to 247 feet per second (the velocity at which choking occurred at the lean fuel-air-ratio limit) caused a gradual decrease in the lean operating range from about 0.064 to 0.074. Increasing V_2 from 170 to 220 feet per second caused no appreciable change in the rich limit of operation. For velocities greater than 220 feet per second, no data were taken at fuel-air ratios greater than about 0.09 because of the low combustion efficiency.

Flame blow-out occurred when p_2 was reduced below 1460 pounds per square foot absolute at a V_2 of about 280 feet per second and a fuel-air ratio of 0.09. At these conditions, the combustion-chamber-outlet Mach number was subsonic and very close to 1.0. At a V_2 of about 160 feet per second, however, stable combustion was obtained over the full fuel-air-ratio range at values of p_2 equal to about 1100 pounds per square foot absolute. The combustion-chamber-outlet Mach number for these conditions was about 0.82. The tunnel static pressure was approximately the same for both conditions, 650 and 620 pounds per square foot absolute, respectively.

The operational limits of the ram jet with the zero-pitch wide-slot burner are shown in figure 7(c). Over a range of V_2 from 230 to 280 feet per second, the operable range of fuel-air ratios extended from about 0.046 to 0.090. Choking at the combustion-chamber outlet occurred at a V_2 of approximately 260 feet per second.

When the zero-pitch wide-slot burner was operated at p_2 of 1640 pounds per square foot absolute and p_0 of 970 pounds per square foot absolute, an increase in fuel-air ratio above 0.070

produced a combustion characterized by a hi-pitch Screech instead of the usual low-pitch roaring sound. This phenomenon was accompanied by a reduction in V_2 from 242 to 202 feet per second (fig. 7(c)), which indicates an increase in the efficiency of combustion. The operable range of fuel-air ratios, however, was reduced to a range from 0.060 to 0.080. Although this change in combustion efficiency could be duplicated at the same pressure and velocity conditions, it was not observed at any of the other combinations of combustion-chamber conditions investigated.

Effect of fuel-air ratio on combustion efficiency and gas total-temperature ratio. - Combustion efficiency η_b and gas total-temperature ratio τ are presented as functions of fuel-air ratio in figures 8 and 9, respectively, for the two-pitch standard-slot burner and the zero-pitch wide-slot burner. Indicated on the figures are the values of p_2 and the range of V_2 at which the data were obtained.

Increases from the leanest to the richest attainable fuel-air ratio caused a steady decrease in η_b . For both burners, the value of τ reached a maximum in the range of the stoichiometric fuel-air ratio. For normal combustion at a V_2 of about 205 feet per second and a fuel-air ratio of 0.075, a τ of 6.0 and an η_b of 74 percent were obtained with the two-pitch standard-slot burner as compared with a τ of 4.7 and an η_b of 52 percent obtained at the same fuel-air ratio and V_2 with the zero-pitch wide-slot burner (figs. 8(c), 8(d), 9(c), and 9(d)). When screeching combustion was obtained with the zero-pitch wide-slot burner at these conditions, however, η_b increased approximately 20 percent with a concomitant increase in τ to 6.2.

Effect of combustion-chamber-inlet velocity on combustion efficiency and gas total-temperature ratio. - The effect of V_2 on η_b and τ are shown in figures 10 and 11, respectively, for the two-pitch standard-slot burner and the zero-pitch wide-slot burner. Indicated on the figures are the values of p_2 and the range of fuel-air ratios over which the data were taken.

With the two-pitch standard-slot burner, η_b improved with increases in V_2 to about 200 feet per second and further increases

1074

in V_2 caused η_b to decrease. The improvement in η_b was presumably due to better atomization and mixing of air with the fuel than at the lower V_2 values. At velocities greater than about 200 feet per second, the decreased time available for combustion within the ram jet probably decreases η_b more rapidly than η_b is increased by improved atomization and mixing of the fuel with air.

A similar variation in τ with V_2 occurred. The largest observed τ of 6.7 was obtained at a fuel-air ratio of about 0.073 and a V_2 of 179 feet per second (fig. 11(a)).

With the zero-pitch wide-slot burner, η_b data were obtained only at a V_2 greater than about 195 feet per second. As with the two-pitch standard-slot burner, η_b declined with increases in V_2 in this range of V_2 . The effects of screeching combustion on η_b and τ previously discussed are shown in figure 10(d) and 11(b), respectively.

Ram-Jet Internal-Flow Characteristics

Some of the flow characteristics through the engine with a two-pitch standard-slot burner and a $17\frac{1}{2}$ -inch combustion-chamber-outlet diameter are presented in figures 12 to 16. The flow characteristics shown in figures 12 to 14 are at an average combustion-chamber-inlet Reynolds number of 1,290,000 (based on a combustion-chamber diameter of 18 in.) for values of τ of 1.0, 4.3, and 5.4. The radial location of the fuel-injector tube and the approximate mean fuel radius are shown in figure 12.

A small qualitative difference between profile of dynamic pressure q in the subsonic diffuser upstream of the fuel-injector tube was obtained for the conditions with and without burning (fig. 12). At the combustion-chamber inlet, a marked change of the profile compared with those upstream of the fuel-injector tube and with those with and without burning was obtained (fig. 13). In general, the profile at the combustion-chamber inlet indicates the growth of a large boundary layer or wake at the wall of the center body extending about halfway across the diffuser-outlet annulus. The additions of heat appeared to accentuate the growth of the center-body wake presumably because the heat added first in the vertex of the perforated conical flame holder tends to force the flow of incoming air toward the perforations nearer the outer wall.

~~CONFIDENTIAL~~

Values of static and total pressures across the combustion chamber 1/2 inch upstream of the ram-jet outlet are presented in figure 14. For the condition without burning, the distribution of total and static pressures is relatively flat. When burning takes place, a marked peak in total and static pressures in the central region of the jet occurs. The minimum total and static pressures occur approximately 2 inches from the combustion-chamber wall. The same general variation of total and static pressures across the combustion chamber for choked and unchoked conditions is indicated in figure 15.

From the values of total and static pressures in figure 15, the variation of Mach number across the jet was computed by assuming a constant ratio of specific heat γ of 1.3 (fig. 16). Inasmuch as the pressure tube of the rake extended approximately 1/2 inch upstream of the outlet of the ram jet, the integrated average of this computed Mach number profile is less than the average ultimate exhaust-jet Mach number M_j computed from the average exhaust-jet total pressure and ambient static-pressure data. For both choked and unchoked conditions at the ram-jet outlet, figure 16 shows a maximum in the Mach number at the center of the jet with a decrease in Mach number toward the combustion-chamber walls.

Over-All Ram-Jet Performance

The variations with equivalent free-stream Mach number M_0 of the parameters jet thrust F_j , reduced jet thrust F_j/δ , total-pressure ratio across engine P_j/P_0 , ultimate exhaust-jet Mach number M_j , reduced specific fuel consumption $W_f/F_n \sqrt{\theta}$, and net-thrust coefficient C_F are shown in figures 17 to 22 for the engine operating with the zero-pitch wide-slot burner and the two-pitch standard-slot burner with and without an orifice plate attached to the combustion-chamber outlet.

Jet thrust is shown as a function of M_0 in figure 17 for the various configurations. When these data were reduced to standard NACA atmospheric conditions at sea level, the reduced jet thrust F_j/δ as a function of M_0 was obtained (fig. 18). At a given M_0 , the higher F_j/δ obtained when the zero-pitch wide-slot burner was used instead of the two-pitch standard-slot burner indicates that the pressure losses through the zero-pitch wide-slot burner are less than through the two-pitch standard-slot burner. The cold pressure-drop coefficient A_p/q_2 for the two-pitch standard-slot flame

holder was 1.5 (reference 4). The lowest value of $F_j/8$ at a given value of M_0 was obtained with the two-pitch standard-810t burner in the ram jet equipped with an orifice plate because of the smaller outlet area A_4 .

Total-pressure losses through the ram jet were reduced when the orifice plate was attached to the combustion-chamber outlet (fig. 19). This reduction in total-pressure loss is primarily the result of the lower value of dynamic pressure through the unit obtained when A_4 is reduced. At M_0 of 1.4, the total-pressure ratio across the unit P_j/P_0 was 0.83 for the ram jet with the two-pitch standard-slot burner with orifice plate, 0.73 with the zero-pitch wide-slot burner with no orifice plate, and 0.70 with the two-pitch standard-slot burner with no orifice plate.

The variation of the ultimate exhaust-jet Mach number M_j is presented in figure 20 as a function of M_0 . Choking at the ram-jet exhaust outlet was obtained at an M_0 of 1.09 when an orifice plate was attached to the combustion-chamber outlet and at an M_0 of 1.25 when no orifice plate was used. The decrease in M_j at a given M_0 when the orifice plate was removed from the combustion-chamber outlet is largely a result of the accompanying increase in total-pressure losses through the ram jet.

A comparison of the minimum value of reduced specific fuel consumption $W_f/F_n \sqrt{\theta}$ (fig. 21) at an M_0 of about 1.4 shows that a reduction in this parameter from about 5.0 to 3.0 pounds of fuel per hour per pound of net thrust was obtained by reducing the combustion-chamber-outlet area with the orifice plate. This improvement in specific fuel consumption was obtained as a result of a reduction in total-pressure losses through the ram jet and an improvement in η_p . (See figs. 7 and 10.) No curves are shown in figure 21 because variations in both τ and η_p caused the data to scatter.

All configurations gave values of thrust coefficient; C_F above 0.6 at an M_0 of 1.4 (fig. 22). Although the net thrust theoretically decreases with decreases in A_4 , a reduction in net thrust at M_0 equal to 1.4 was not obtained when the orifice plate was attached because of decreased pressure losses and increased τ . The maximum value of C_F was 0.68 at M_0 of 1.44 and τ of 6.1 for the ram jet with the orifice plate and the two-pitch standard-slot burner (fig. 22(a)).

SUMMARY OF RESULTS

The following results were obtained from an investigation of the performance of a Bumblebee 18-inch ram jet with various can-type burners using kerosene as fuel:

1. The performance of the following two can-type burner configurations was better than that of the other burner configurations investigated: (1) a flame holder having a two-pitch alignment of perforations, 0.07-inch-wide cooling slots, and an arrangement of fuel nozzle8 providing a mean fuel radius of 7.24 inches, and (2) a flame holder having a zero-pitch alignment of perforations, 0.16-inch-wide cooling slots, and a similar arrangement of fuel nozzles providing a mean fuel radius of 6.89 inches. At choking conditions, the operable fuel-air ratio range for the two-pitch standard-slot burner was from 0.074 to greater than 0.090. With a $14\frac{3}{4}$ -inch orifice plate attached to the ram-jet outlet, the operable fuel-air ratio range at choking condition8 for this burner was 0.048 to 0.098. The zero-pitch wide-slot burner gave an operable fuel-air-ratio range from about 0.045 to 0.090 at choking condition8 with no Orifice plate attached to the ram-jet outlet.

2. For the two best burner configurations investigated, the value of gas total-temperature ratio at a given combustion-chamber-inlet velocity reached a maximum at approximately the stoichiometric fuel-air ratio. At a combustion-chamber-inlet velocity of about 205 feet per second and a fuel-air ratio of 0.075, a gas total-temperature ratio of 6.0 and a combustion efficiency of 74 percent were obtained With the two-pitch standard-slot burner as compared with a total-temperature ratio of 4.7 and a combustion efficiency of 52 percent obtained with the zero-pitch wide-slot burner. At a given value of fuel-air ratio, increases in combustion-chamber-inlet velocity greater than about 200 feet per second caused the combustion efficiency and the gas total-temperature ratio to decrease for both burners.

3. At a ram pressure ratio equivalent to a free-stream Mach number of 1.44 and a pressure altitude of 30,000 feet, the minimum reduced specific fuel consumption attained was 3.0 pounds of fuel per hour per pound of net thrust for the unit employing the burner having a flame holder with a two-pitch alignment of

perforations and the $14\frac{3}{4}$ -inch-diameter orifice plate attached to the combustion-chamber outlet. A maximum value of net thrust coefficient Of 0.68 was also attained with this configuration at the same conditions of equivalent free-stream Mach number and altitude.

Lewis Flight Propulsion Laboratory,
National Advisory Committee for Aeronautics,
Cleveland, Ohio.

REFERENCES

1. Anon.: Survey of Bumblebee Activities. Bumblebee Series Rep. No. 69, Appl. Phys. Lab., Johns Hopkins Univ., Oct. 1947. (U. S. Navy Contract NOrd 7386.)
2. Wilcox, Fred A., and Howard, Ephraim M.: Comparison of Two Fuel8 in Bumblebee 18-Inch Ram Jet Incorporating Rake-Type Flame Holder. NACA RM No. E8F11, 1946.
3. Howard, Ephraim M., Wilcox, Fred A., and Dupree, David T.: Combustion-Chamber Performance with Four Fuel8 in Bumblebee 18-Inch Ram Jet Incorporating Various Rake- or Gutter-Type Flame Holders. NACA RM No. E8I01a, 1948.
4. Sterbentz, W. H., and Nussdorfer, T. J.: Investigation of Performance of Bumblebee 18-Inch Ram Jet with a Can-Type Flame Holder. NACA RM No. E8E21, 1948.
5. Anon.: Bumblebee Equipment Manual. Bumblebee Series Rep. No. 62, Appl. Phys. Lab., Johns Hopkins Univ., Nov. 1947. (U. S. Navy Contract NOrd 7386.)
6. Perchonok, Eugene, Wilcox, Fred A., and Sterbentz, William H.: Preliminary Development and Performance Investigation of a 20-Inch Steady-Flow Ram Jet. NACA ACR No. E6D05, 1946.
7. Perchonok, Eugene, Sterbentz, William H., and Wilcox, Fred A.: Performance of a 20-Inch Steady-Flow Ram Jet at High Altitude8 and Ram-Pressure Ratios. NACA RM No. E6L06, 1947.

TABLE I - SUMMARY OF PERFORMANCE OF VARIOUS BURNER CONFIGURATIONS

Configuration	Flameholder			Over-all fuel-injection pattern		Ram-jet-outlet diameter (in.)	Conditions of operation			
	Open area percent)	Pitch	Cooling-slot width (in.)	Basic patterns used alternately	Mean fuel radius (in.)		Burning	Ram-jet-outlet choking	Approximate range of operation	
									Combustion-chamber-inlet static pressure, p_2 lb/sq ft abs.	Approximate fuel-air ratio f/a
1	130	0	0.07	4 and 3P (tube 5 plugged in pattern 3P)	7.20	$17\frac{1}{2}$	Rough	Unobtainable	1200-2000	0.060-0.080
2	110	0	.07	4 and 3P (tube 5 plugged in pattern 3P)	7.20	$17\frac{1}{2}$	Stable	Not determined	2000	.068 - .078
3	130	2	.07	4 and 3P (tube 5 plugged in pattern 3P)	7.20	$17\frac{1}{2}$	Rough	Unobtainable	950-2000	.041 - .083
4	130	2	.07	4 and 3P	6.89	$17\frac{1}{2}$	--do---	----do----	1800-2000	.050 - .069
5	130	2	.07	4 and 3P (tubes 1 and 5 plugged in pattern 3P)	7.24	$14\frac{3}{4}$	Stable	Obtainable	1100-2000	(See fig. 7(a))
6	130	2	.07	4 and 3P (tubes 1 and 5 plugged in pattern 3P)	7.24	$17\frac{1}{2}$	--do---	----do----	1100-2000	(See fig. 7(b))
7	130	2	.07	4 and 4A (tubes 1 and 2 plugged in pattern 4A)	7.37	$17\frac{1}{2}$	--do---	----do----	1500-2000	0.075-0.092
8	135	0	.16	4 and 3P	6.89	$17\frac{1}{2}$	--do---	----do----	1100-2000	(See fig. 7(c))



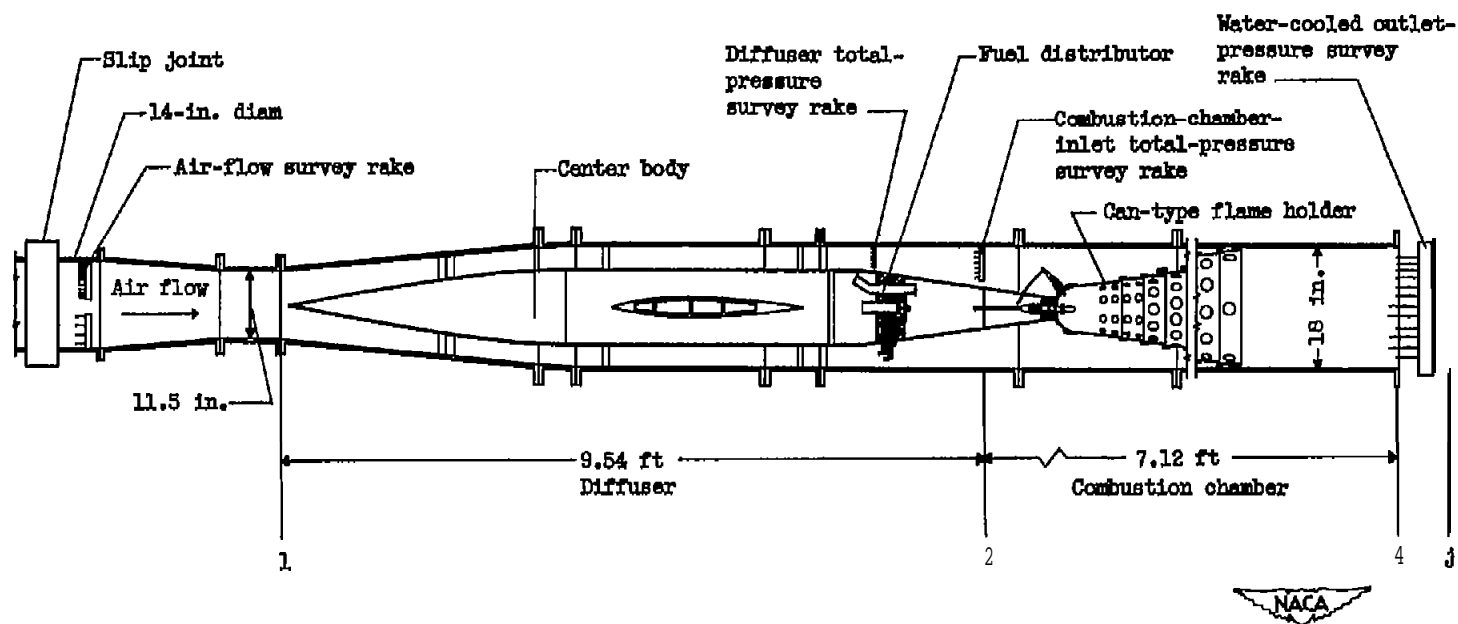


Figure 1. - Schematic diagram of Bumblebee 18-inch ram jet showing instrumentation.

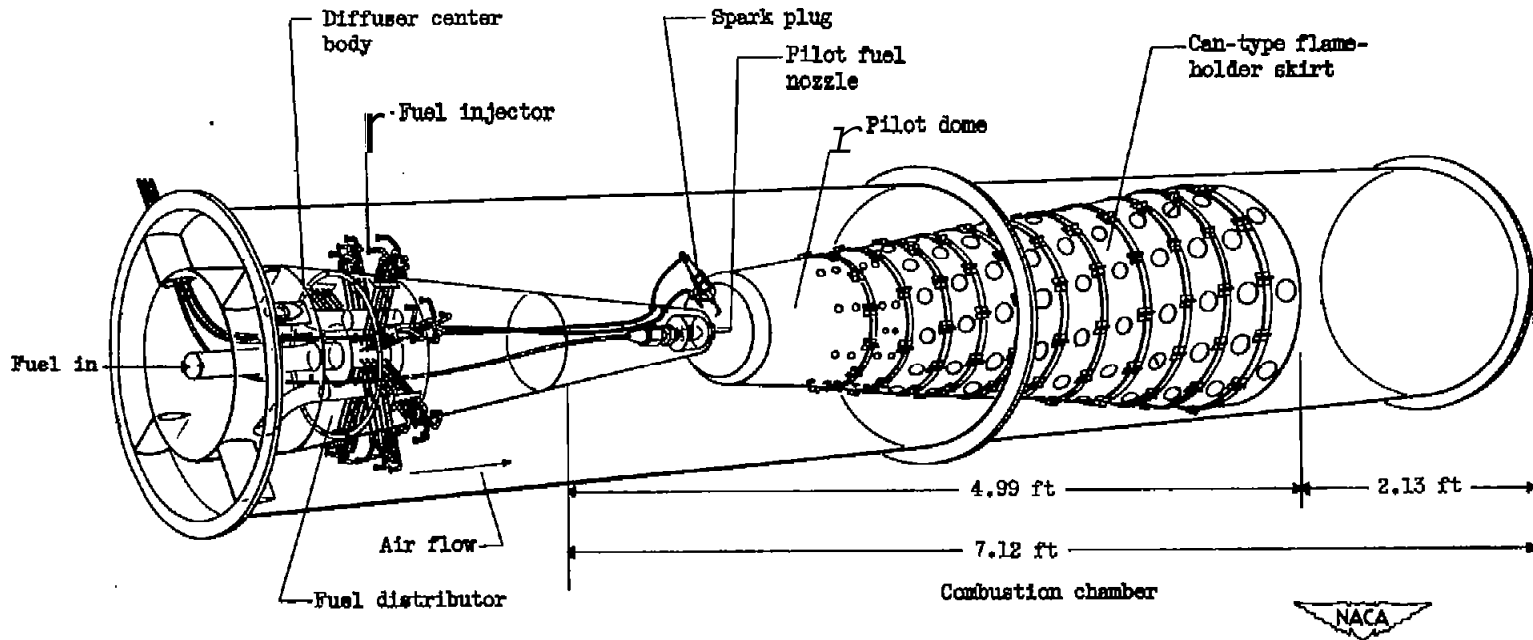
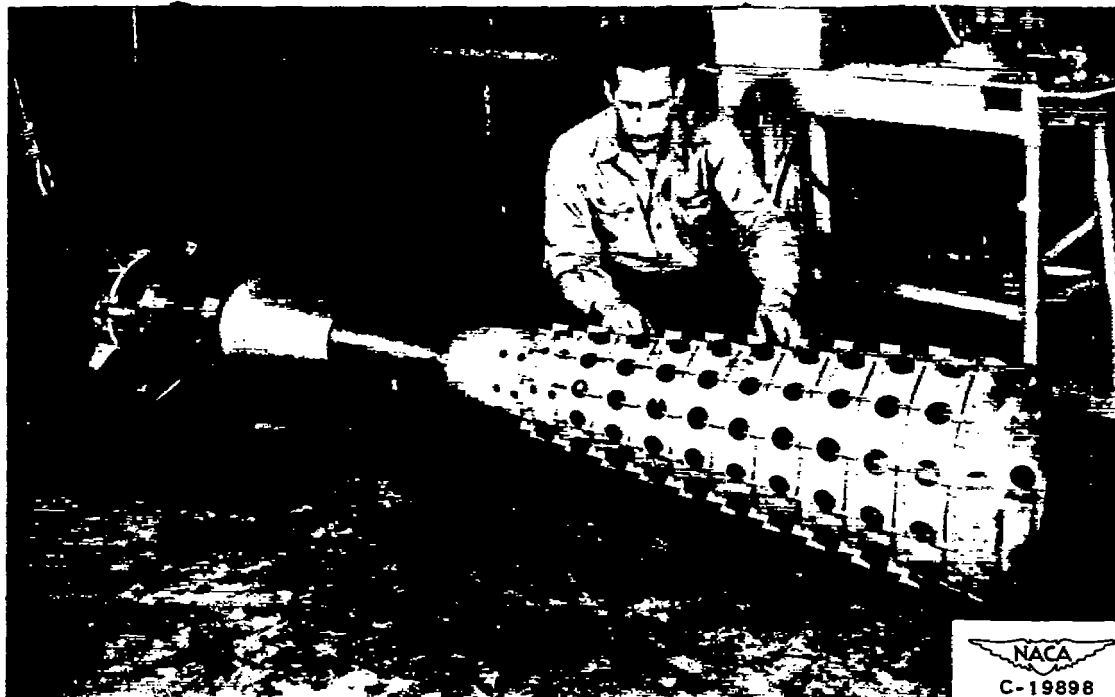
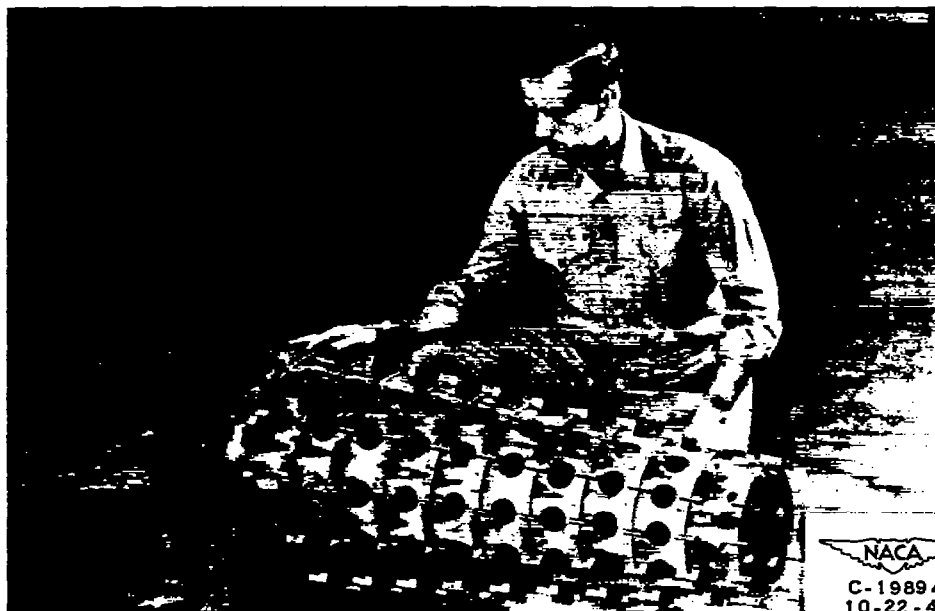


Figure 2. - Schematic diagram of installation of fuel distributor and flame holder.



NACA
C-19898
10-22-47

(a) Zero-pitch alignment of perforations, 0.07-inch cooling slots, and 110-percent open area. Pilot dome attached to diffuser center body and skirt.



NACA
C-19894
10-22-47

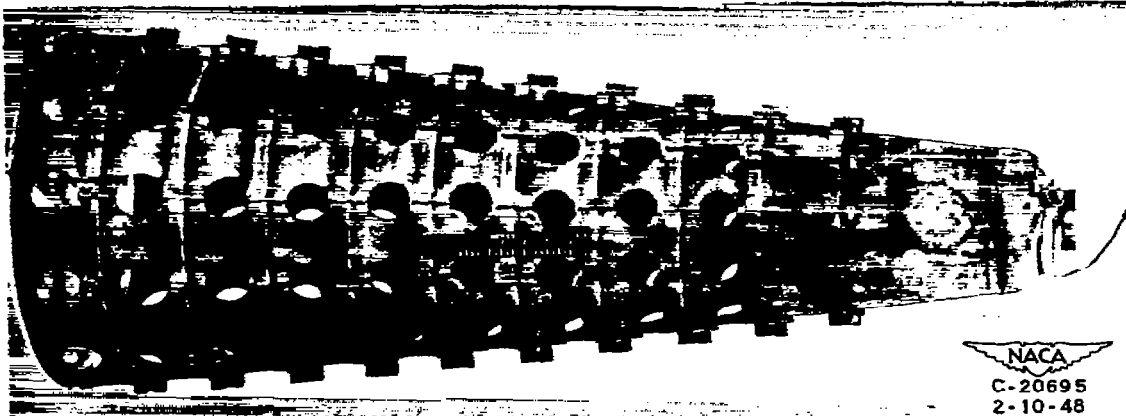
(b) Zero-pitch alignment of perforations, 0.07-inch cooling slots, and 130-percent open area.

Figure 3. - Can-type flame-holder skirts.

██████████

██████████

1074



(c) Zero-pitch alignment of perforations, 0.16-inch cooling slots, and 135-percent open area. Pilot dome attached to skirt.



(d) Two-pitch alignment of perforations, 0.07-inch cooling slots, and 130-percent open area.

Figure 3. - Concluded. Can-type flame-holder skirts.

11-11-11

.

11-11-11

161-1303

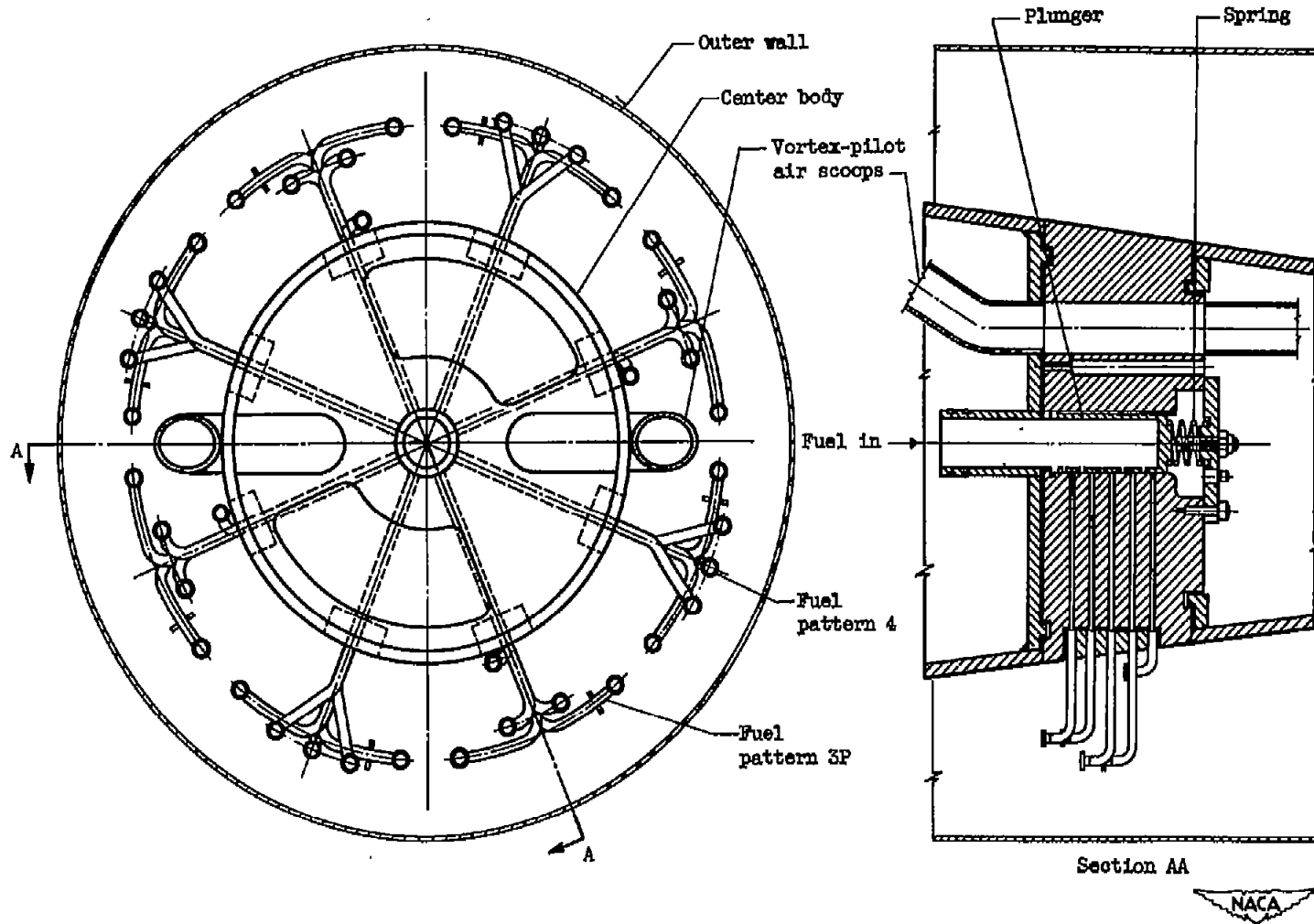
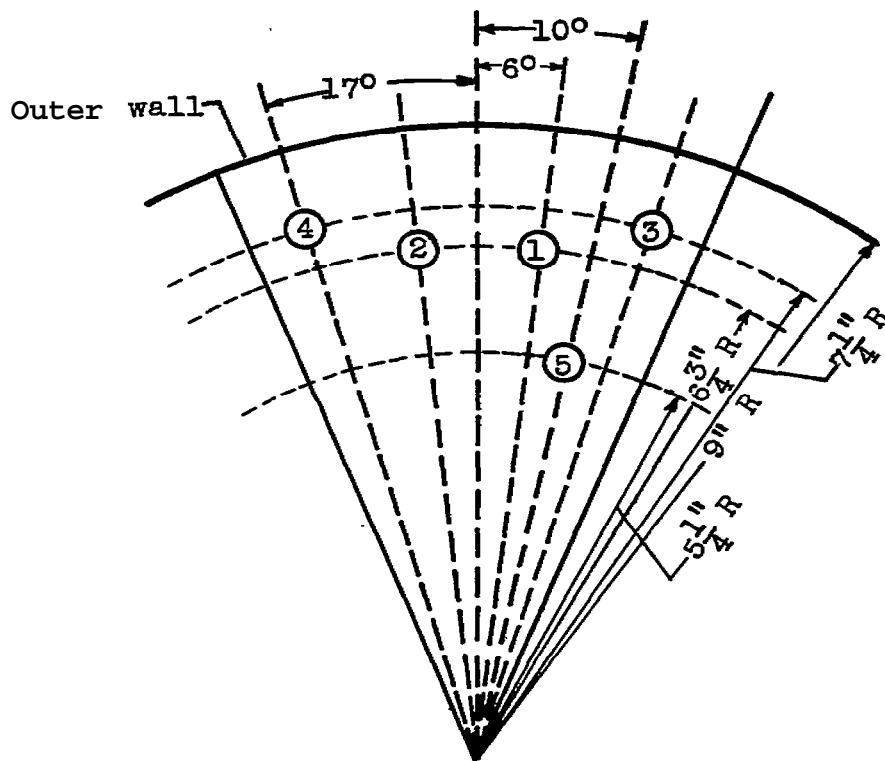
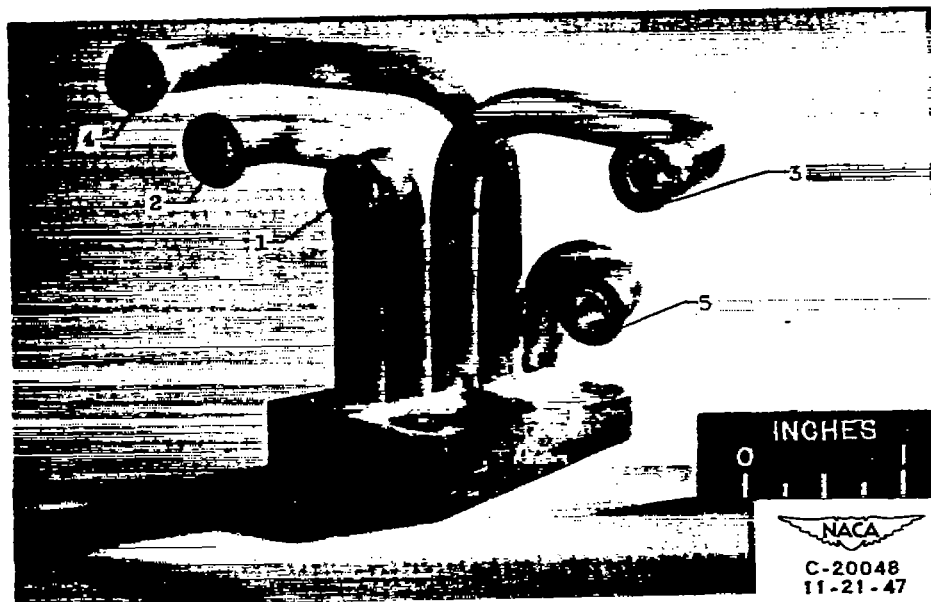


Figure 4. - Schematic diagram of fuel distributor with typical over-all fuel-injector pattern.



(a) Fuel pattern 3P.

Figure 5. - Photographs and schematic diagrams of basic fuel patterns.

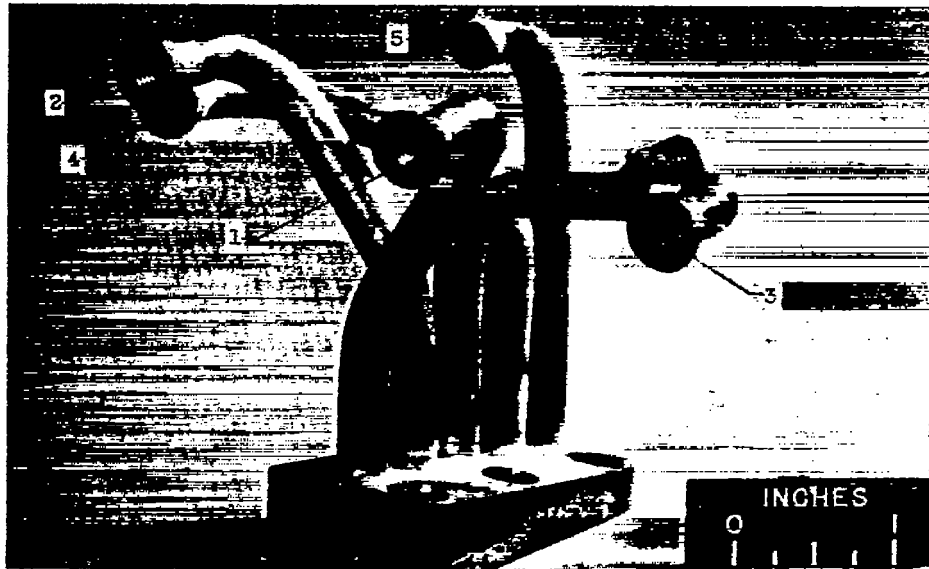
████████████████████

.

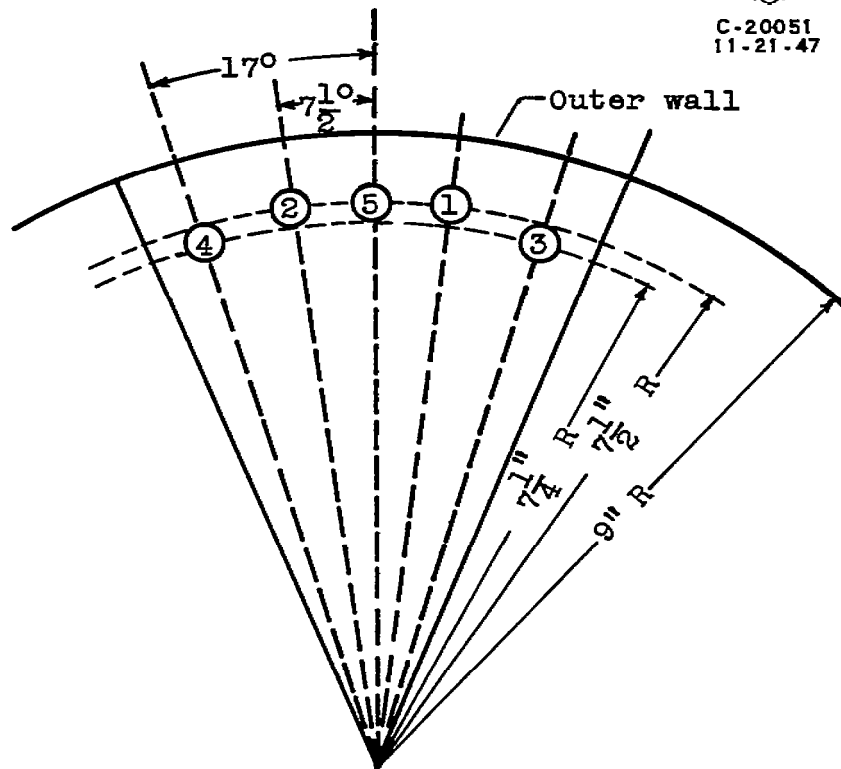
.

.

████████████████████



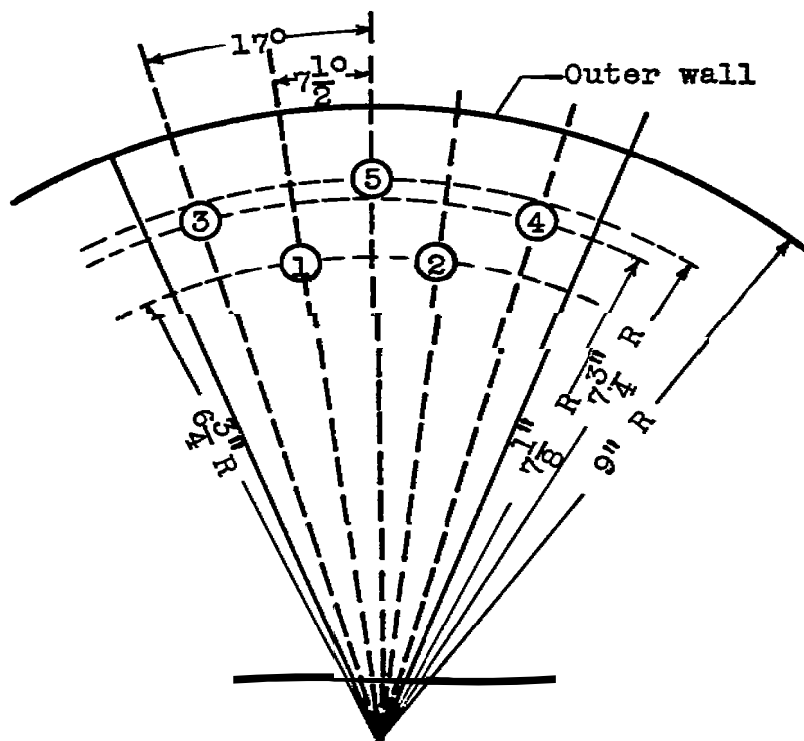
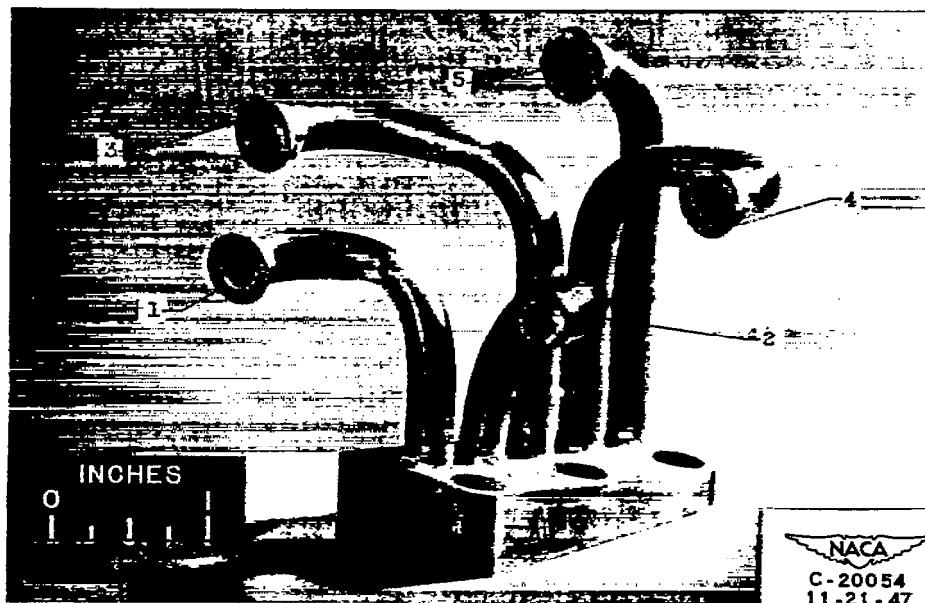
NACA
C-20051
11-21-47



(b) Fuel pattern 4.

Figure 5. - Continued. Photographs and schematic diagrams of basic fuel patterns.

1074



(c) Pattern number 4A.

Figure 5. - Concluded. Photographs and schematic diagrams of basic fuel patterns.

██████████

██████████

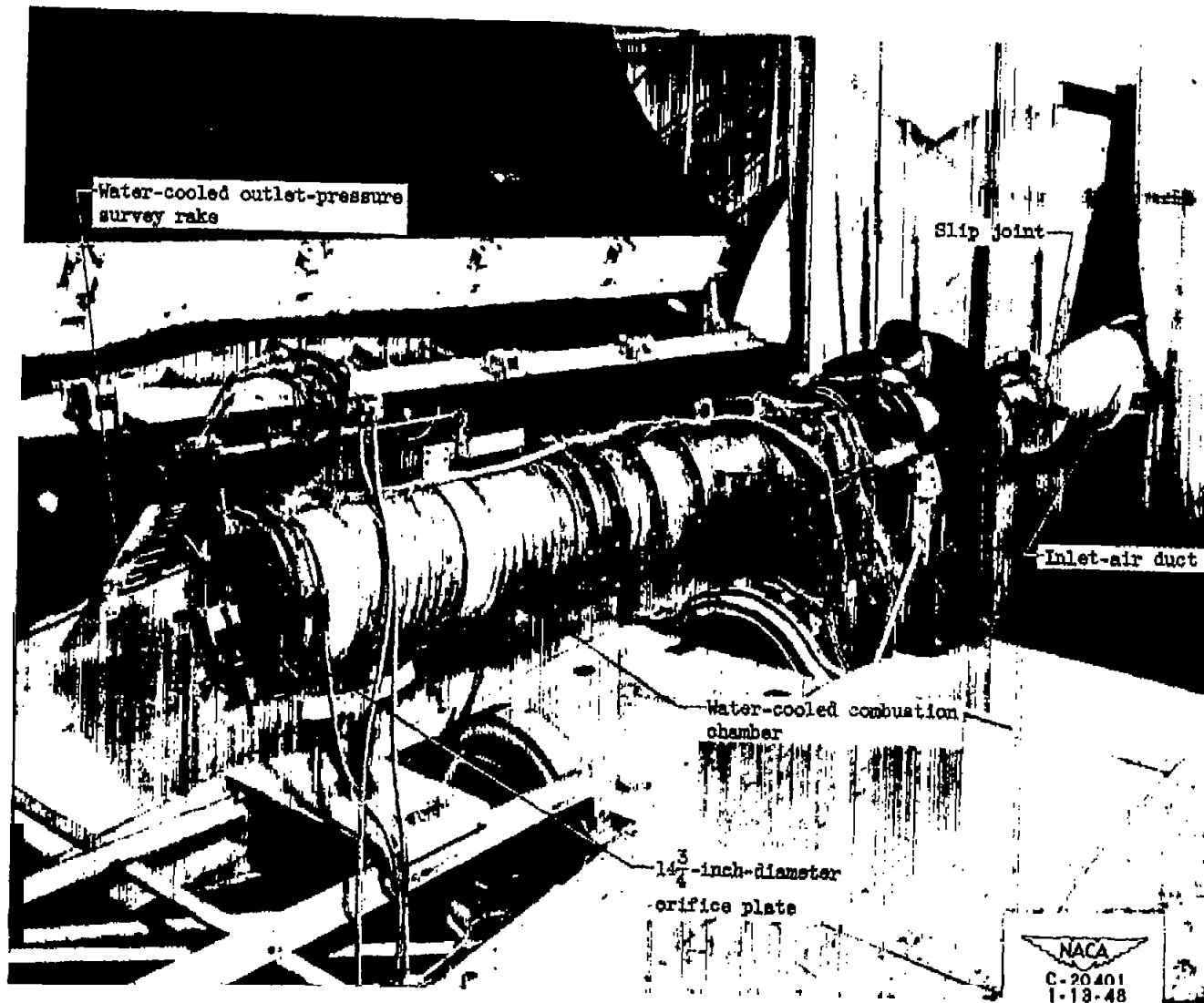


Figure 6. - Installation of Bumblebee 18-inch ram jet in altitude wind tunnel.

SECRET

SECRET

1074

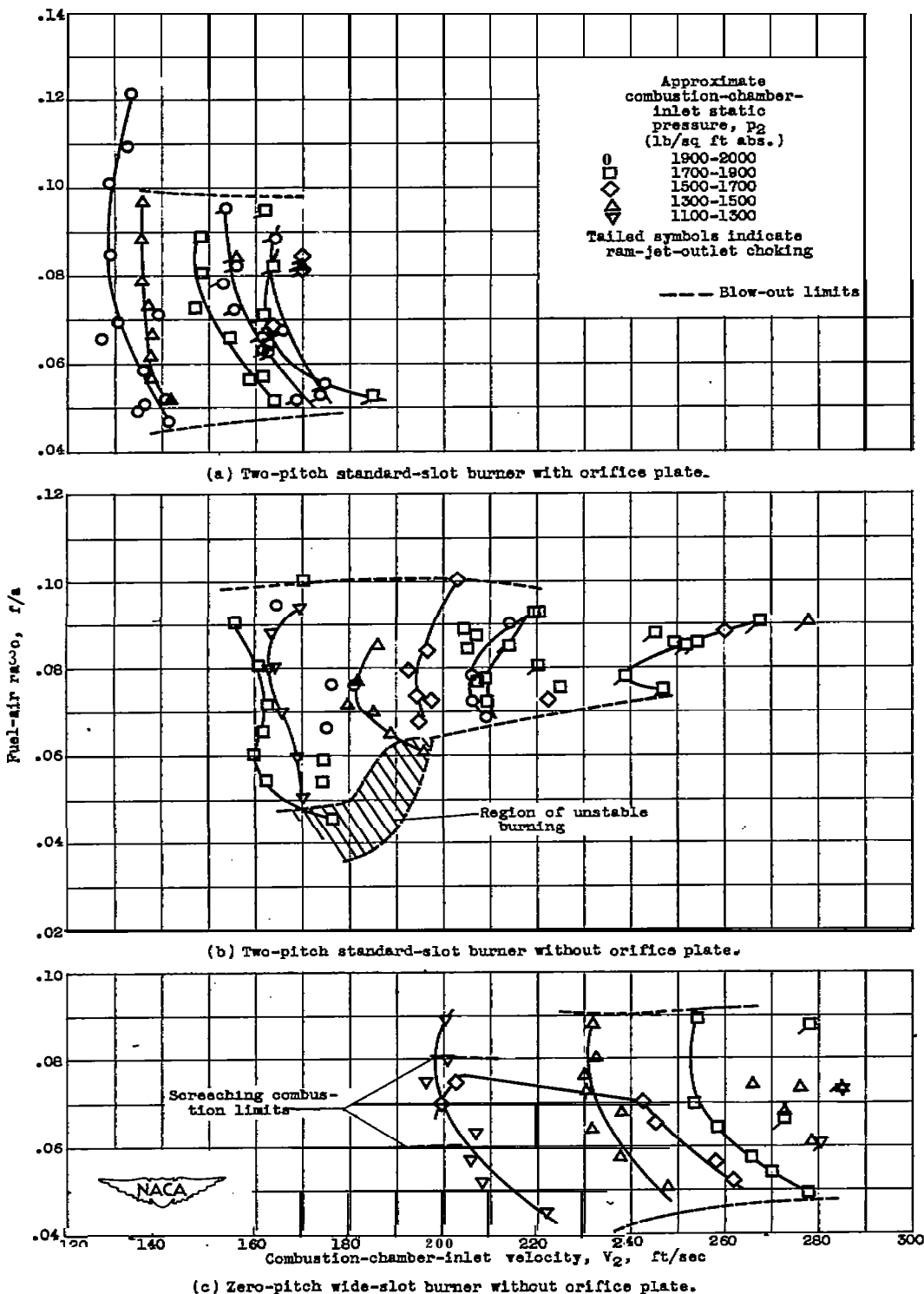


Figure 7. - Fuel-air-ratio operating range as function of combustion-chamber-inlet velocity and pressure. Combustion-chamber-inlet temperature, $140^\circ \pm 10^\circ F$.

~~CONFIDENTIAL~~

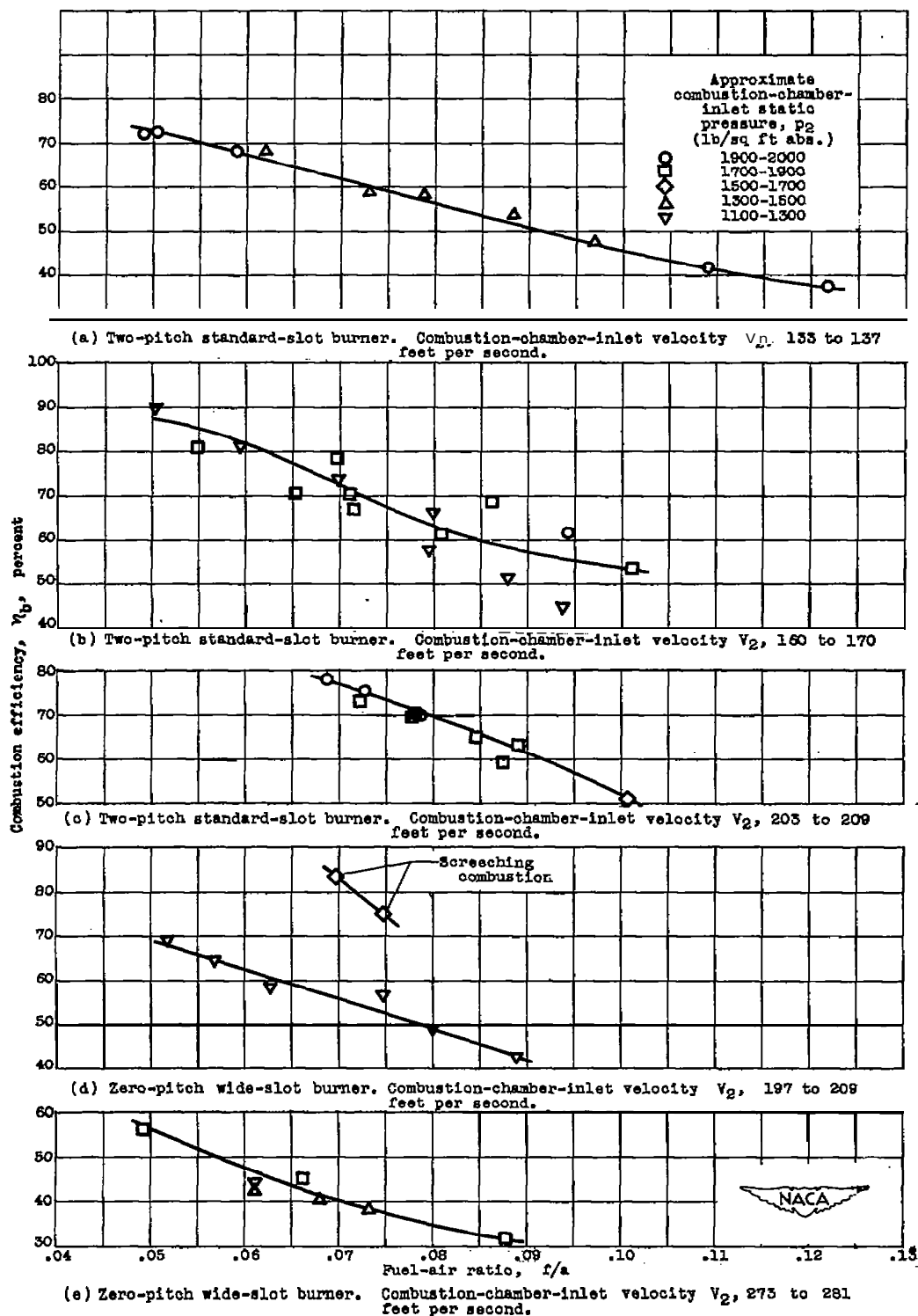


Figure 8. - Effect of fuel-air ratio on combustion efficiency at various combustion-chamber-inlet velocities. Combustion-chamber-inlet temperature, $140^\circ \pm 10^\circ$ F.

1074

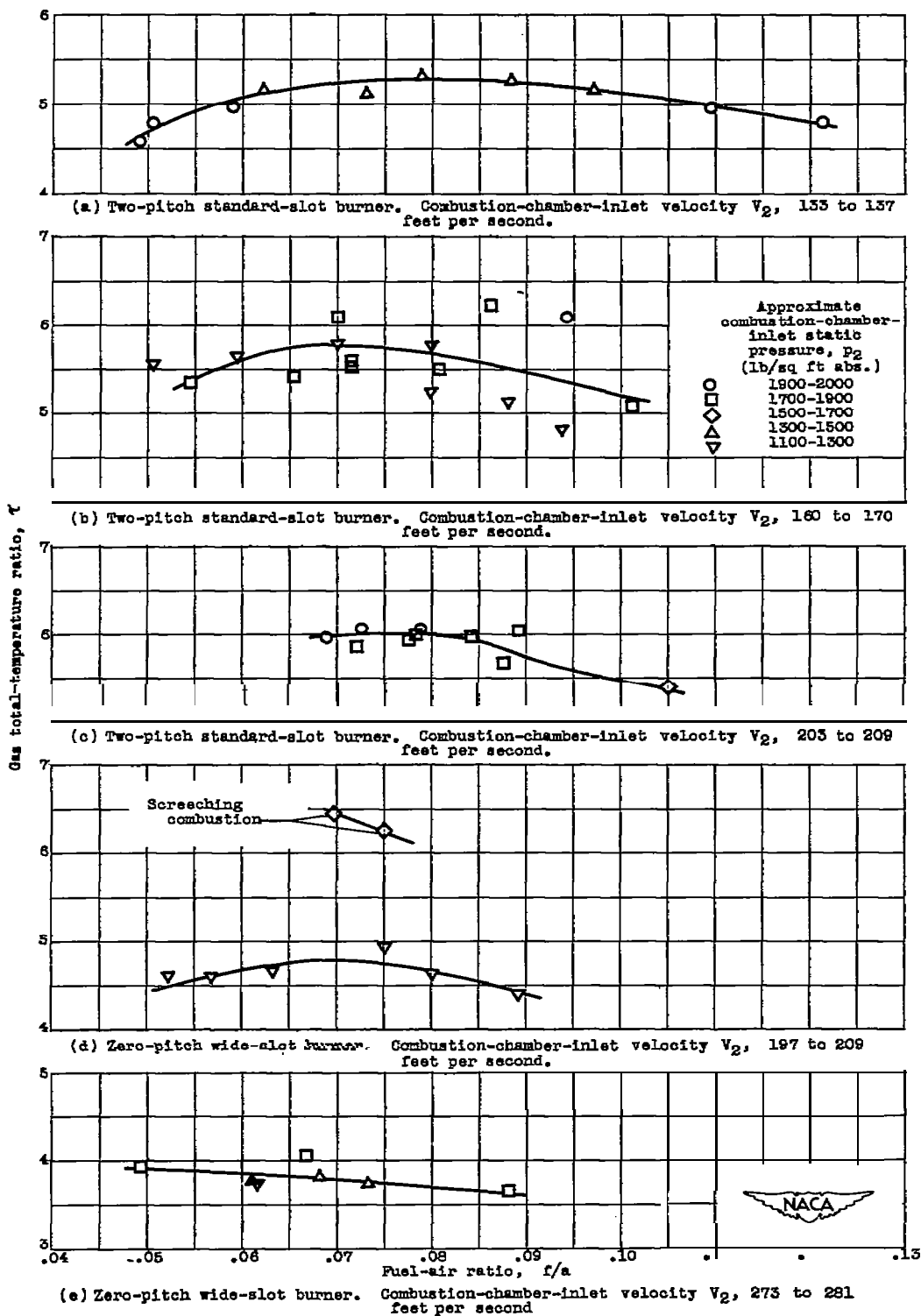


Figure 9. - Effect of fuel-air ratio on gas total-temperature ratio across ram jet at various combustion-chamber-inlet velocities. Combustion-chamber-inlet temperature, $140^\circ \pm 10^\circ$ F.

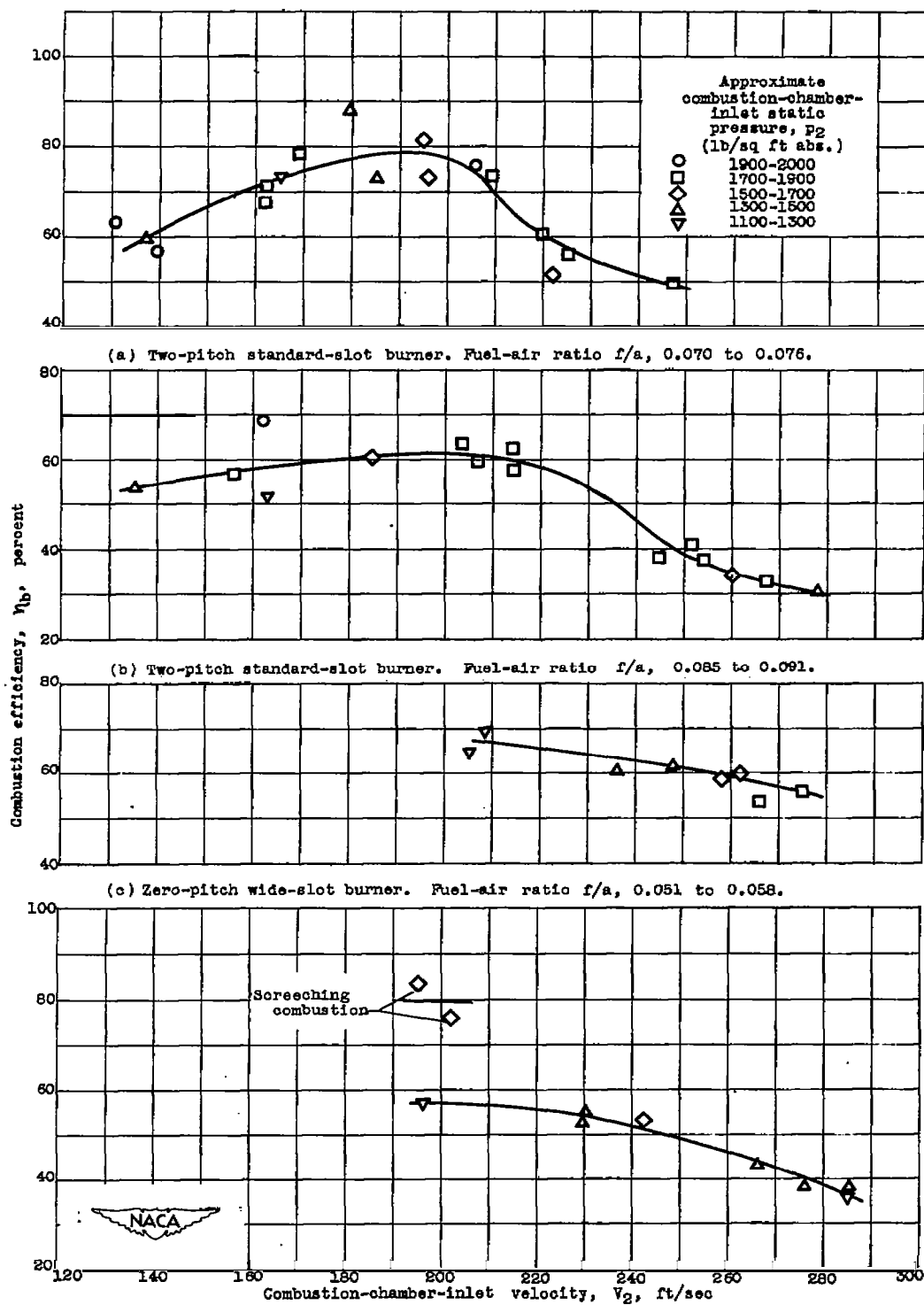


Figure 10. - Effect of combustion-chamber-inlet velocity on combustion efficiency at various fuel-air ratios. Combustion-chamber-inlet temperature, $140^\circ \pm 10^\circ$ F.

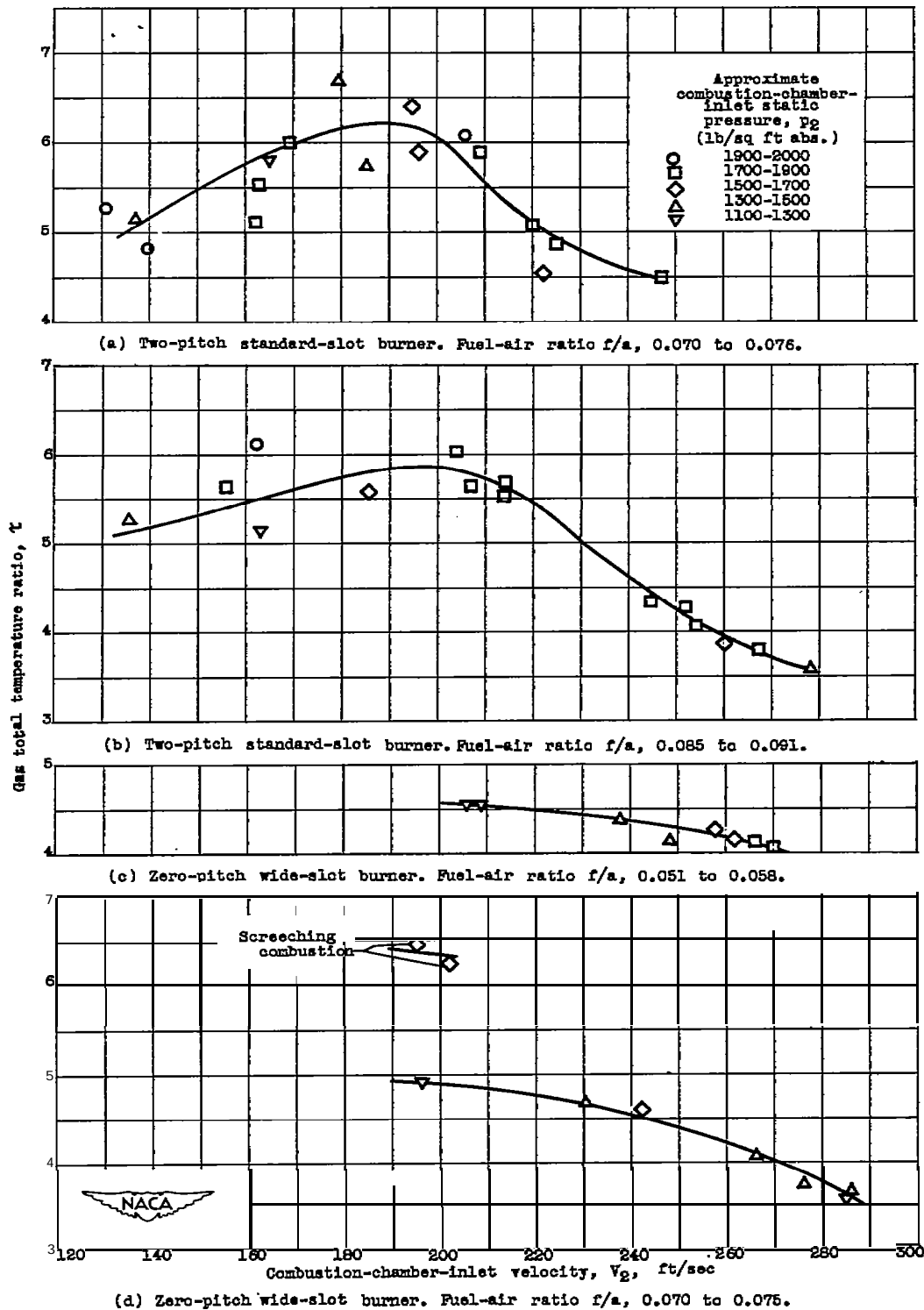


Figure 11. - Effect of combustion-chamber-inlet velocity on combustion efficiency at various fuel-air ratios. Combustion-chamber-inlet temperature, 1400 ± 100 F.

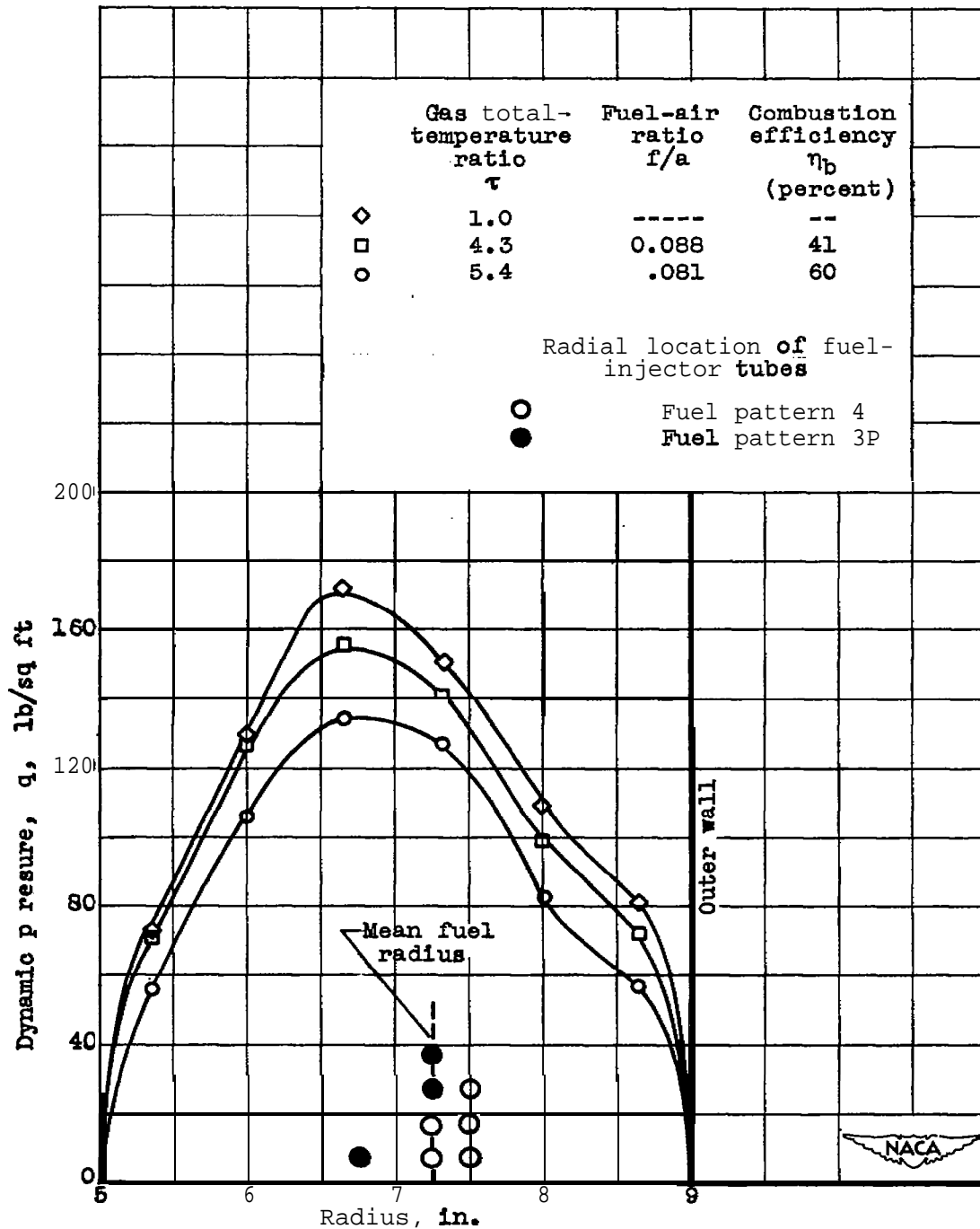


Figure 12. - Profiles of dynamic pressure in subsonic diffuser immediately upstream of fuel injector for various gas total-temperature ratios across ram jet at an average combustion-chamber-inlet Reynolds number of 1,290,000. Two-pitch standard-slot burner; combustion-chamber-outlet diameter, $17\frac{1}{2}$ inches.

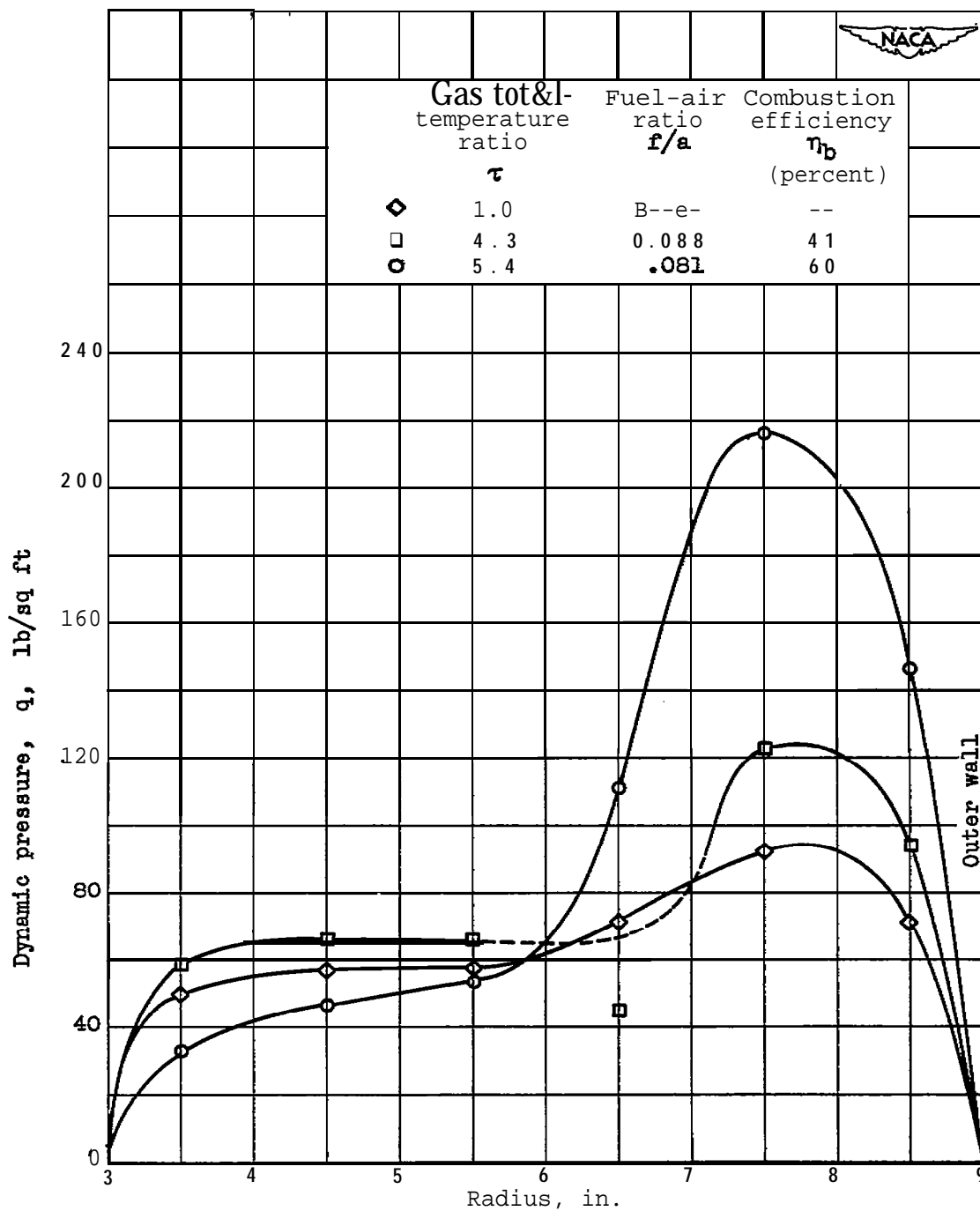


Figure 13. - Profiles of dynamic pressure at combustion-chamber inlet for various gas total-temperature ratios across ram jet at average combustion-chamber-inlet Reynolds number of 1,290,000. Two-pitch standard-slot burner; combustion-chamber-outlet diameter, $17\frac{1}{2}$ inches.

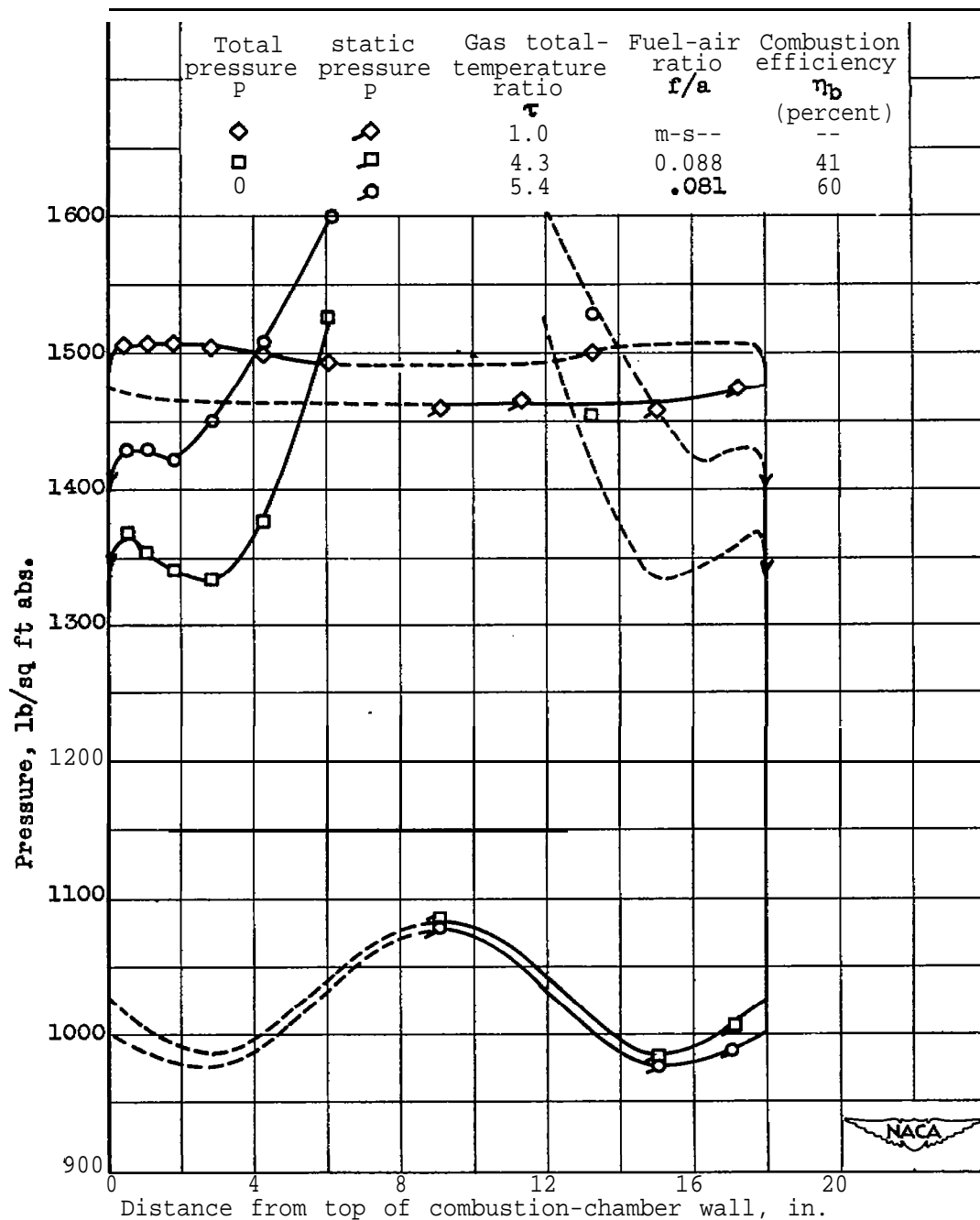


Figure 14. - Profiles of total and static pressures across combustion chamber 1/2 inch upstream of ram-jet outlet for various gas total-temperature ratios across ram jet at average combustion-chamber-inlet Reynolds number of 1,290,000. Two-pitch standard-slot burner; combustion-chamber-outlet diameter, $17\frac{1}{2}$ inches.

074

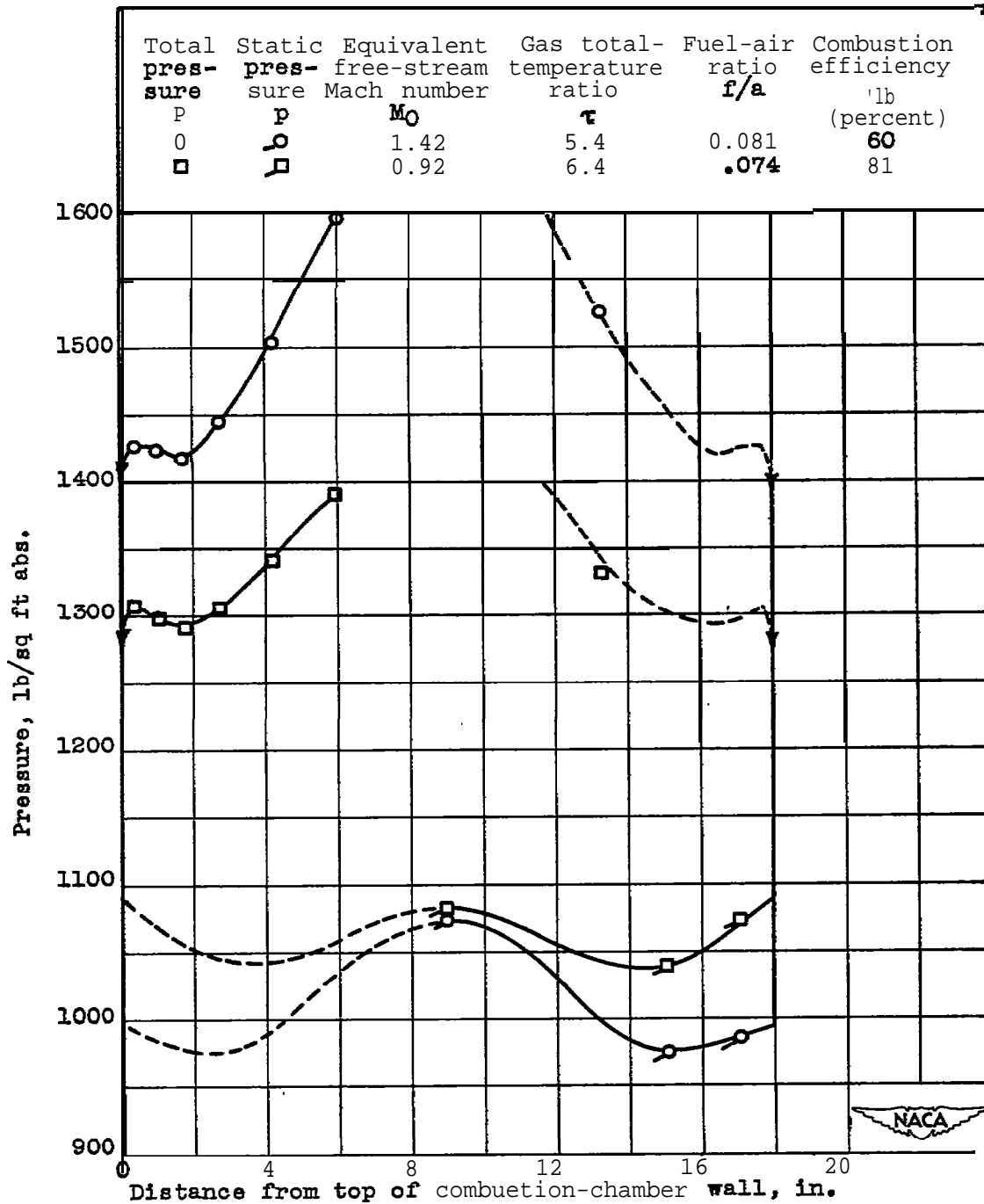


Figure 15. - Profiles of total and static pressures across combustion chamber $1/2$ inch upstream of ram-jet outlet for choked and unchoked conditions at ram-jet outlet. Two-pitch standard-slot burner; combustion-chamber-outlet diameter, $17\frac{1}{2}$ inches.

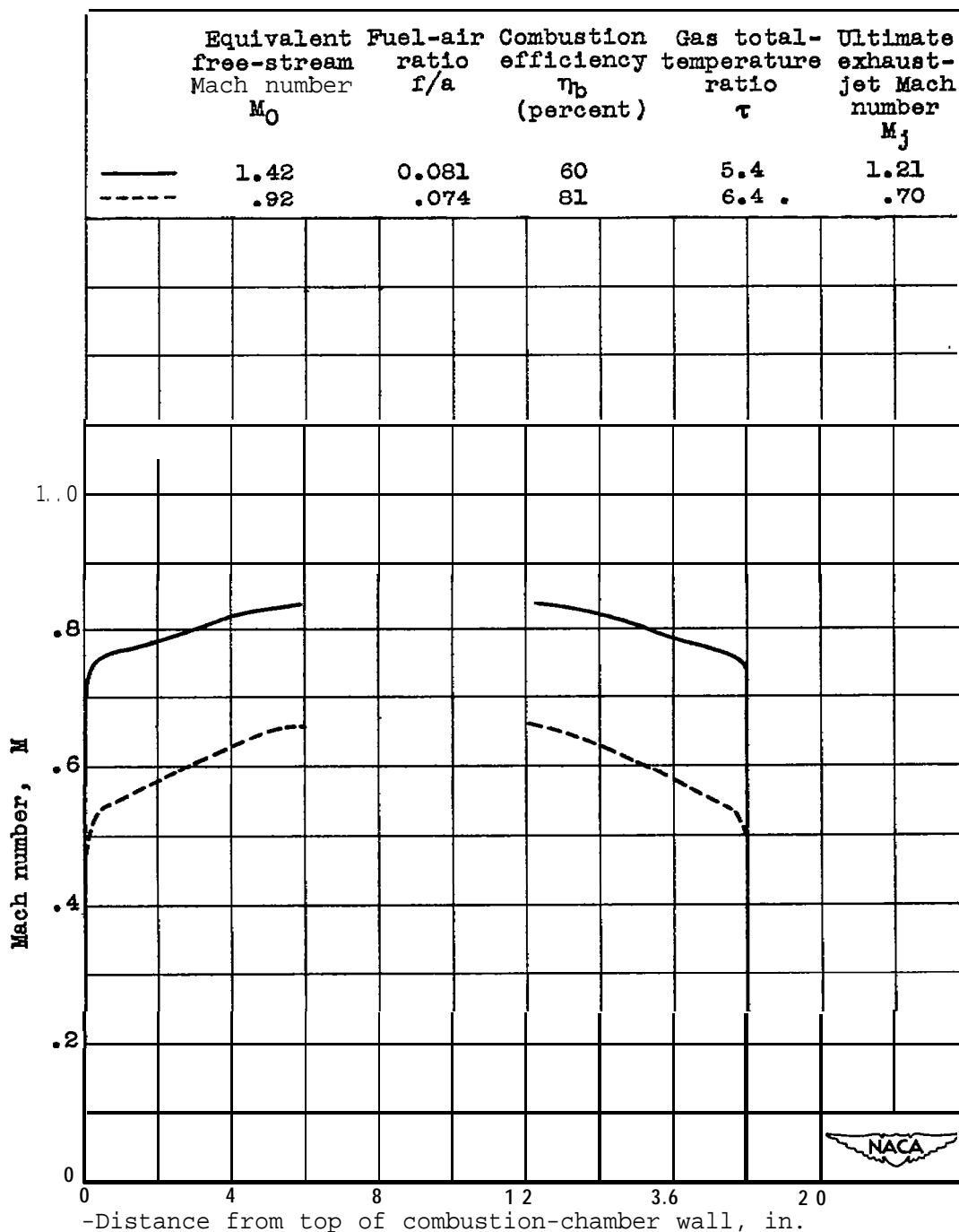


Figure 16. -Profiles of Mach number across combustion chamber $1/2$ inch upstream of ram-jet outlet for choked and **unchoked** conditions at ram-jet outlet. Two-pitch standard-slot burner; combustion-chamber-outlet diameter, $17\frac{1}{2}$ inches; ratio of specific heats, 1.3.

1074

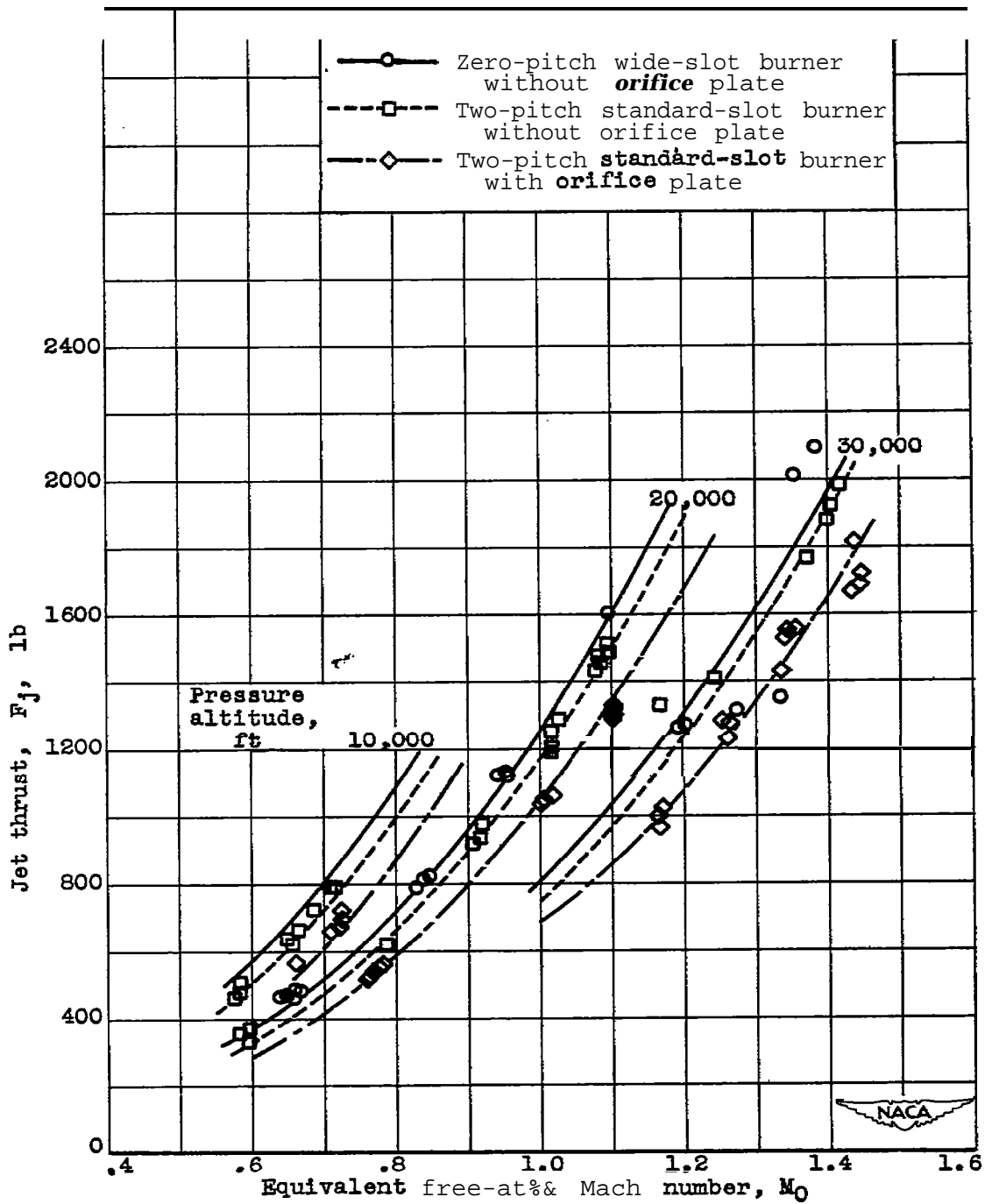


Figure 17. - Effect of equivalent free-stream Mach number and pressure altitude on jet thrust for various ram-jet configurations.

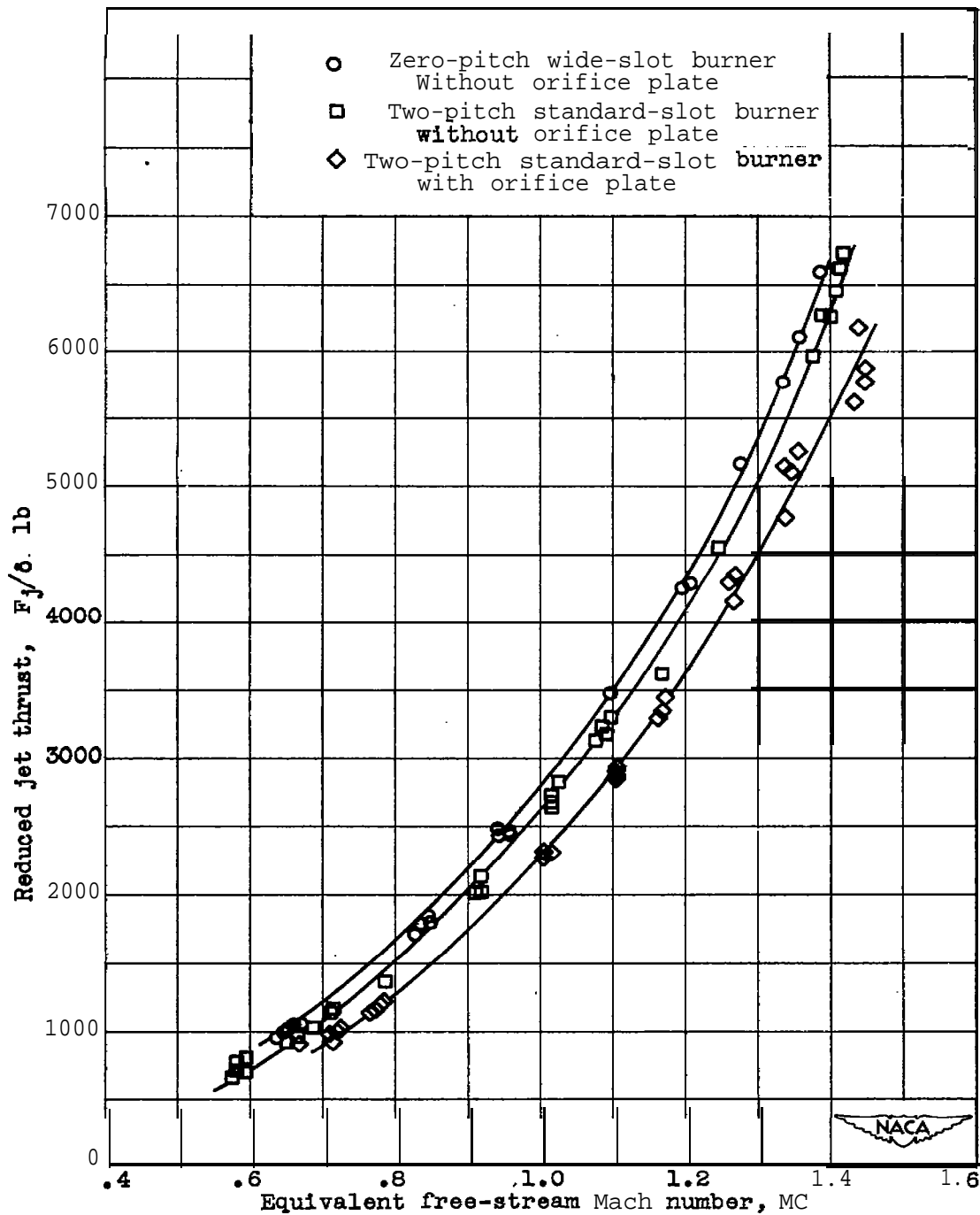


Figure 18. - Effect of equivalent free-stream Mach number on reduced jet thrust for various engine configurations. Jet thrust reduced to NACA standard atmospheric conditions at sea level.

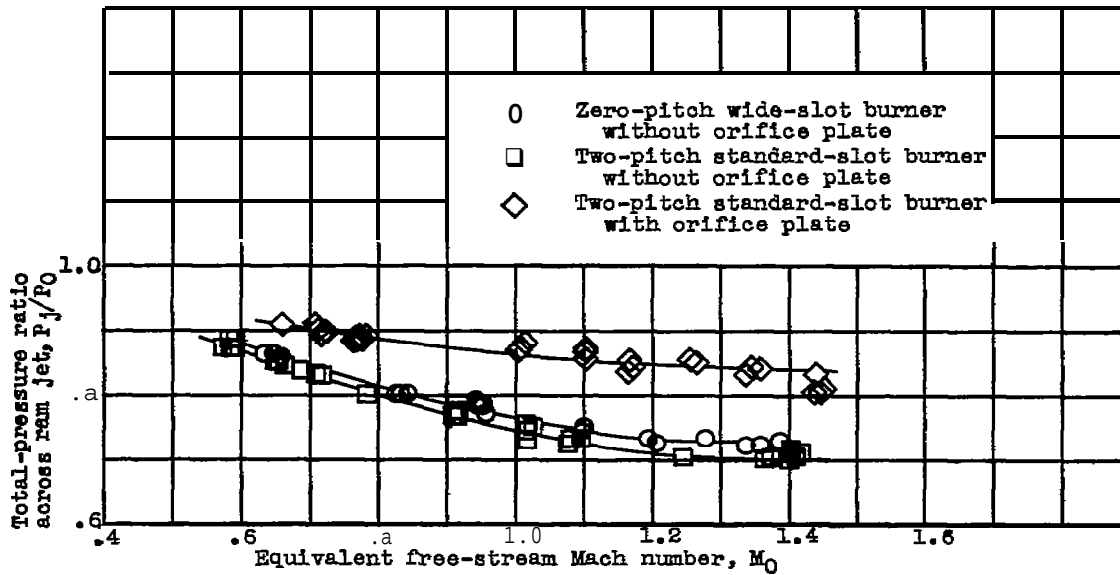


Figure 19. - Effect of equivalent free-stream Mach number on total-pressure ratio across ram jet for various engine configurations.

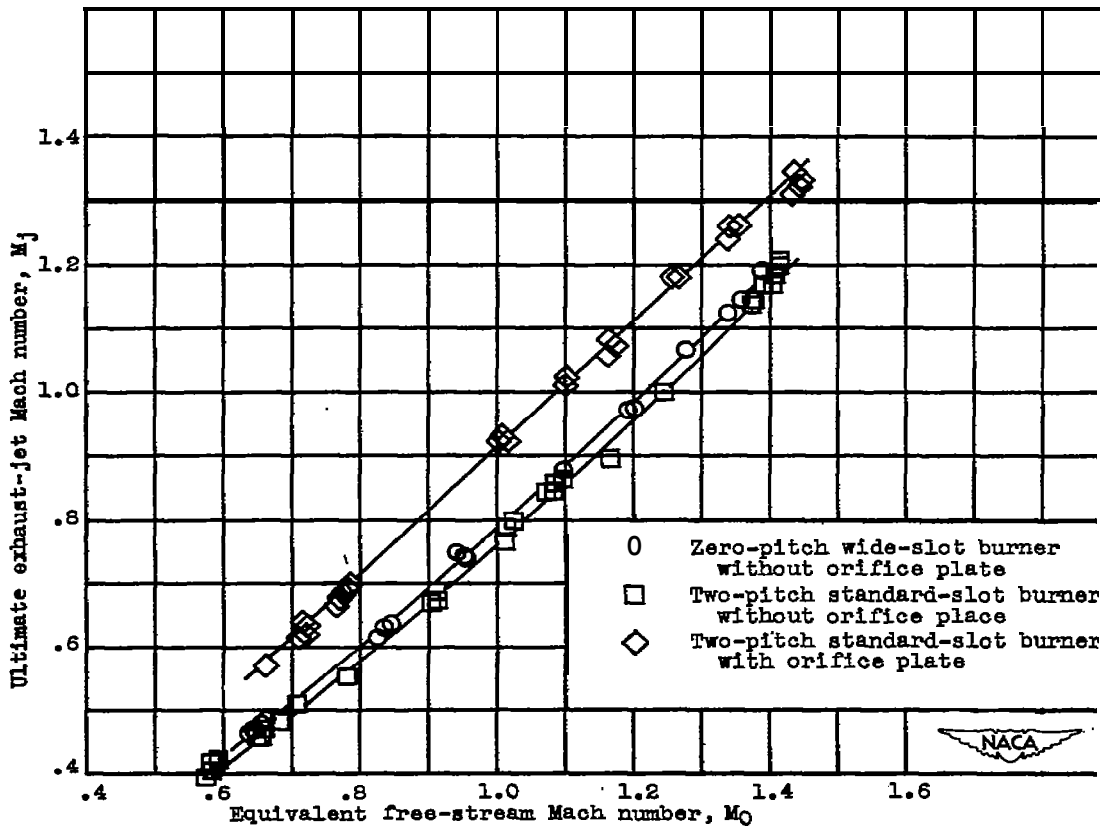


Figure 20. - Effect of equivalent free-stream Mach number on ultimate exhaust-jet Mach number for various engine configurations.

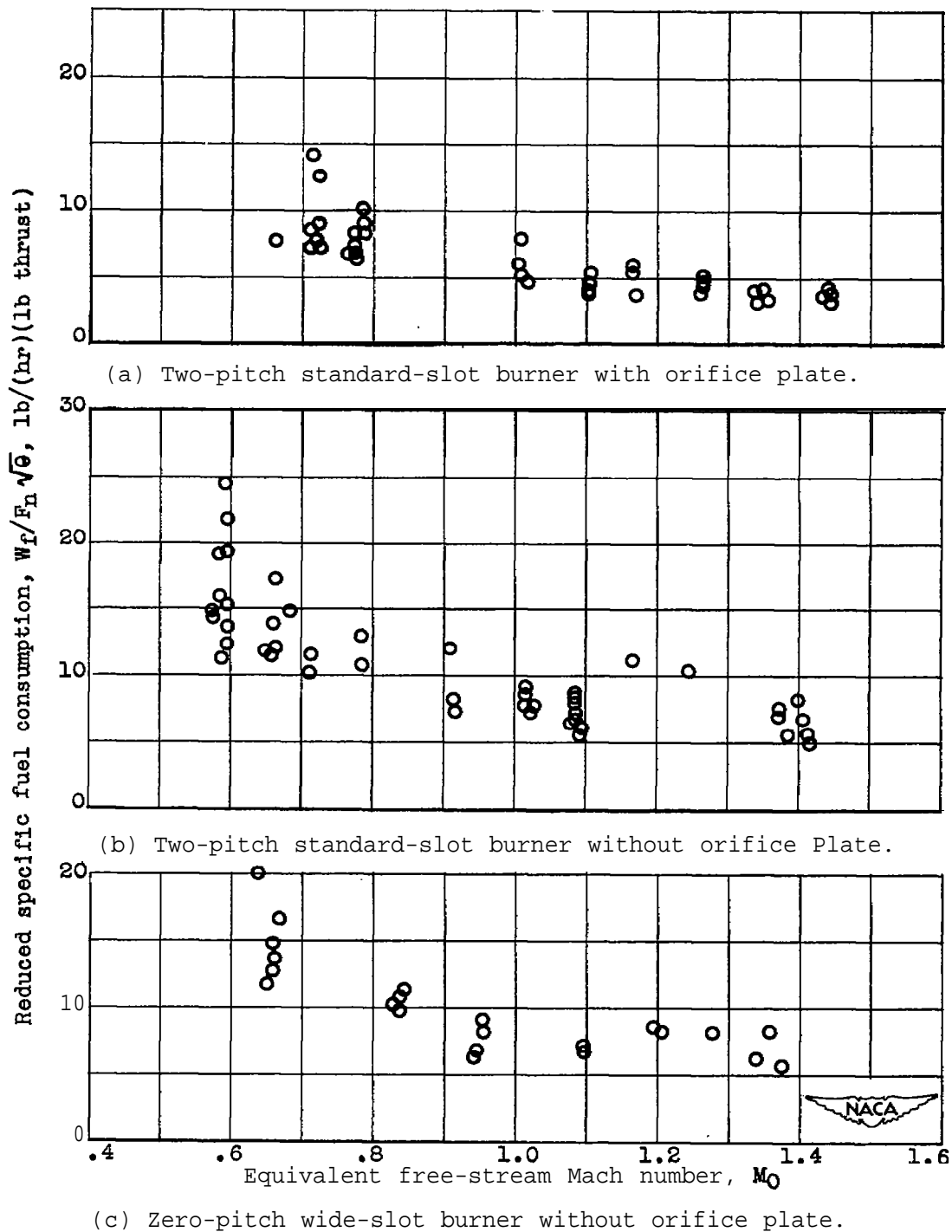
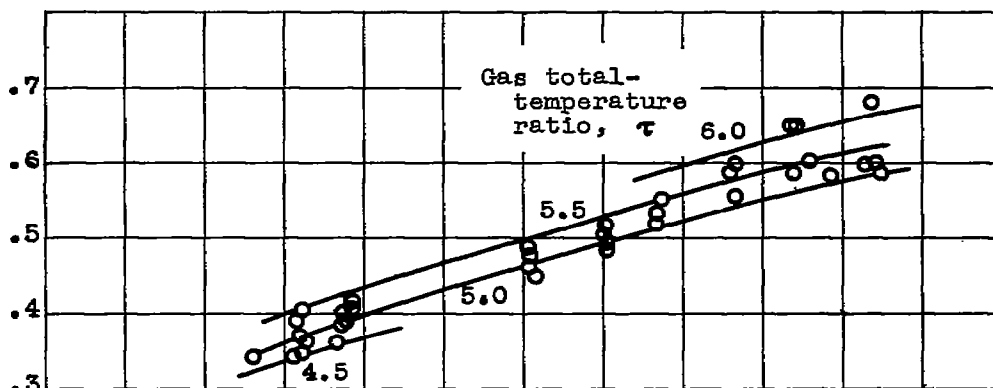
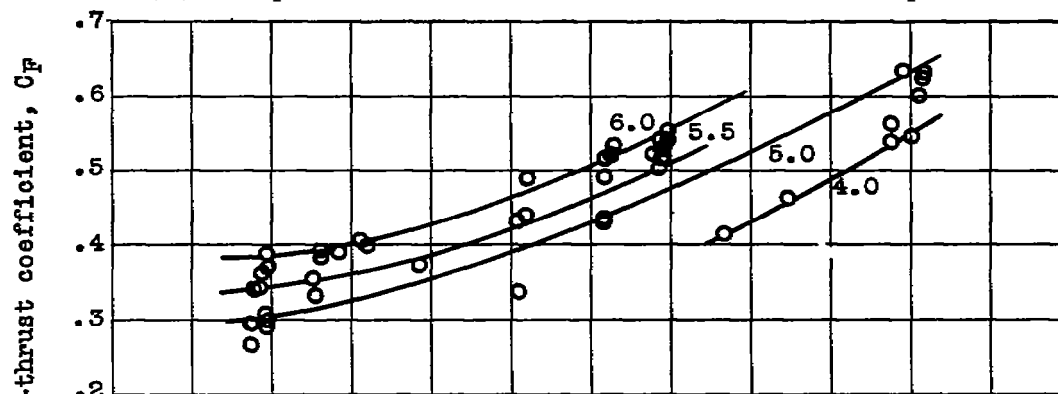


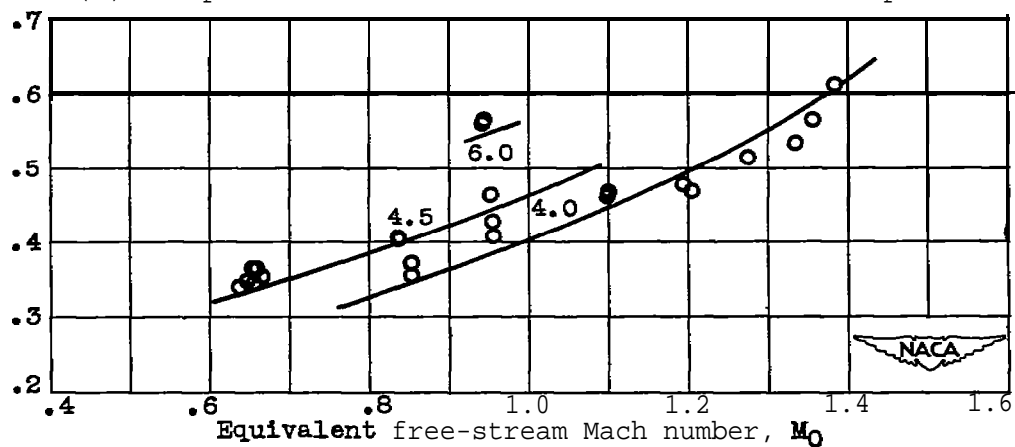
Figure 21. - Effect of equivalent free-stream Mach number on reduced specific fuel consumption for various ram-jet configurations. Specific fuel consumption reduced to NACA standard atmospheric conditions at sea level.



(a) Two-pitch standard-slot burner with orifice plate.



(b) Two-pitch standard-slot burner without orifice plate.



(c) Zero-pitch wide-slot burner without orifice plate.

Figure 22. - Effect of equivalent free-stream Mach number and gas-total temperature ratio on net-thrust coefficient for various ram-jet configurations.

NASA Technical Library



3 1176 01435 0699